

# Radii of Mirror Nuclei and Isobaric Triplets

Ben Ohayon

<sup>a</sup>The Helen Diller Quantum Center, Department of Physics, Technion–Israel Institute of Technology, Haifa 3200003, Israel, [bohayon@technion.ac.il](mailto:bohayon@technion.ac.il)

## Abstract

We present a review of absolute root-mean-square charge radii of stable nuclei up to  $Z = 32$ , which includes a previously overlooked uncertainty in the combined analysis of muonic x-ray and electron scattering experiments. From these *reference radii* and isotope shift measurements, we obtain those of 12 mirror pairs with a traceable and realistic uncertainty budget. The difference in radii between mirror nuclei is found to be proportional to the isospin asymmetry, confirming recent calculations by Novario *et al.* [PRL 130, 032501]. From the fitted proportionality constant and its uncertainty, the radii of 73 previously unknown mirror partners are predicted. These are useful e.g. for benchmarking atomic and nuclear theory, calibrating entire chains, and as an input to nuclear beta-decay calculations. The radii of ( $T = 1, T_z = 0$ ) nuclei are interpolated assuming negligible isospin symmetry breaking. This completes a model-independent, high-precision extraction of the charge and weak radii of all nuclei involved in the testing of the unitarity of the CKM matrix.

## 1. Overview

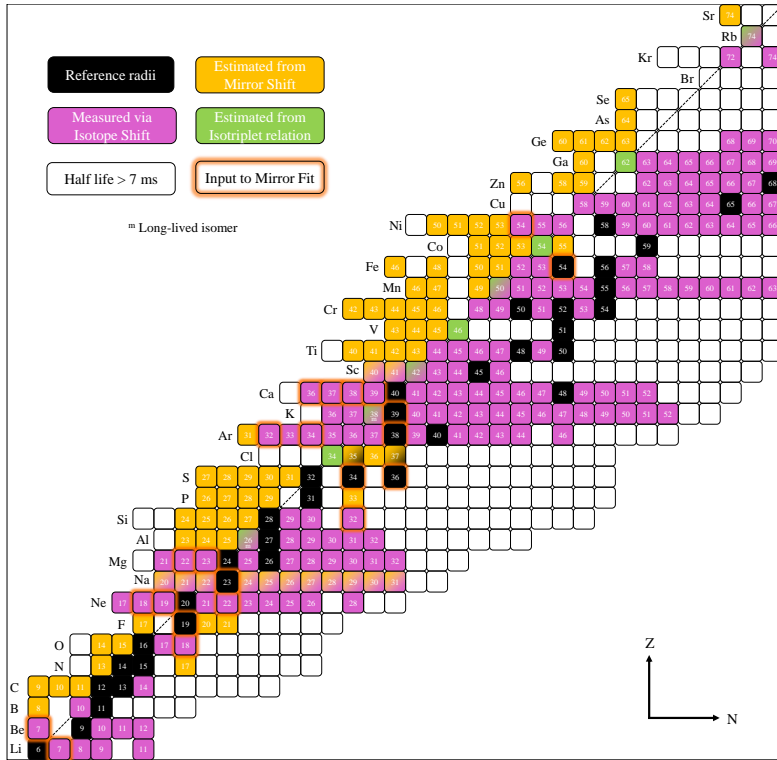


**Fig. 1:** Overview of nuclei relevant to this work, indicated by element name and mass number. Reevaluated reference radii are given in Table 2. The radii of the neon chain are re-estimated in this work and given in Table 3. Radii which are an input to the mirror fit are given in Table 4. Radii measured via isotope shifts are given in Table 5, with those estimated from the mirror shift given in italics. The recalibrated sodium chain is in table 6. Charge and weak radii estimated from the isotriplet relation are given in Table 7.

## 2. Re-evaluation of reference radii

### 2.1. From Barrett to second moments

The backbones of this work are the absolute RMS radii (second moments of the charge distribution) of one or more stable isotope of each element. We refer to them as *reference radii*. These have been predominantly obtained from a combined analysis of elastic electron scattering cross sections, and the energies of x-ray photons emitted in the cascade of muons bound to a nucleus [1] (‘muonic x-rays’). The procedure used in most cases is described in e.g. [2]. First, a Barret equivalent radius (BER),  $R_{k,\alpha}^\mu$ , is extracted from a measured transition energy. The superscript  $\mu$  is there to remind us muonic atoms are used. The parameters  $k \approx 2, \alpha \approx 0$  are calculated for that transition (typically  $2P_{3/2} - 1S$ ) by numerically solving the Dirac equation with some approximate charge distribution [3]. They can be found in [1]. In the spherically symmetric limit,  $R_{k,\alpha}^\mu$  is by construction nuclear charge distribution independent [4], and so in all but a few light stable isotopes from lithium to neon [5], its uncertainty is dominated by that of the nuclear polarization correction to the muonic energy levels.

In order to make the translation from  $R_{k,\alpha}^\mu$  to the more universal RMS charge radius, information on the charge distribution (‘nuclear shape’), from either calculations or elastic electron scattering experiments, is incorporated. It has been noticed that such experiments are particularly well-suited to measure *ratios* of moments, typically with accuracies an order of magnitude higher than integral quantities [4]. Denoting the ratio  $V_2^e = R_{k,\alpha}^e/r^e \approx \sqrt{5/3}$ , with the superscripts to remind us that these quantities are calculated from charge distributions measured in electron scattering, then the RMS radius obtained by a combined analysis reads

$$r^{e\mu} = R_{k,\alpha}^\mu/V_2^e. \quad (1)$$

$r^{e\mu}$  is considered to be highly reliable as it exploits the strength in the two experimental methods while circumventing their weaknesses [4]. However, there are certain limitations to this recipe. The main one is that high-statistics, high momentum-transfer scattering experiments, as well as the individuals who interpret them, are rare, making the applicability of Eq. 1 limited to a subset of the cases. To circumvent this problem, Angeli had fitted an analytical function to a subset of the  $V_2$  factors, averaged on isotopes, making a coarse estimate of the variation  $V_2(Z)$  [6]. The resulting  $V_2$ -factors are only accurate to a few per mill (as stated in Ref. [6]), which translates directly to a similar fractional accuracy in charge radii determined via a combined analysis of Eq. 1. These considerations are absent in later compilations [7, 8], in which no uncertainty in  $V_2(Z)$  is given. To our knowledge, Ref. [9], in which  $r^{e\mu}(^{27}\text{Al})$  is estimated, is the only example in which an uncertainty in  $V_2$  is given. To accomplish this,  $V_2(^{27}\text{Al})$  was estimated from three different scattering experiments [10–12]. The difference between the results is taken as uncertainty, which was found to dominate that of  $r^{e\mu}(^{27}\text{Al})$ . Here we refine and generalize this approach in order to recommend transparent and reliable reference radii.

In light of the above, we now show that the uncertainty in  $V_2$  is dominating for most radii and must be taken into account. At least within the Barret-moment analysis framework. For convenience, we introduce the reduced proportionality factor

$$v = 1 - \sqrt{\frac{3}{5}}V_2^e, \quad (2)$$

which tends to zero for nuclei with a uniform charge distribution. We will see that  $v$  increases from 2 to 9 per mill between  $Z = 6$  and  $Z = 32$ . This means that any extraction of charge radii from muonic x-ray measurements with

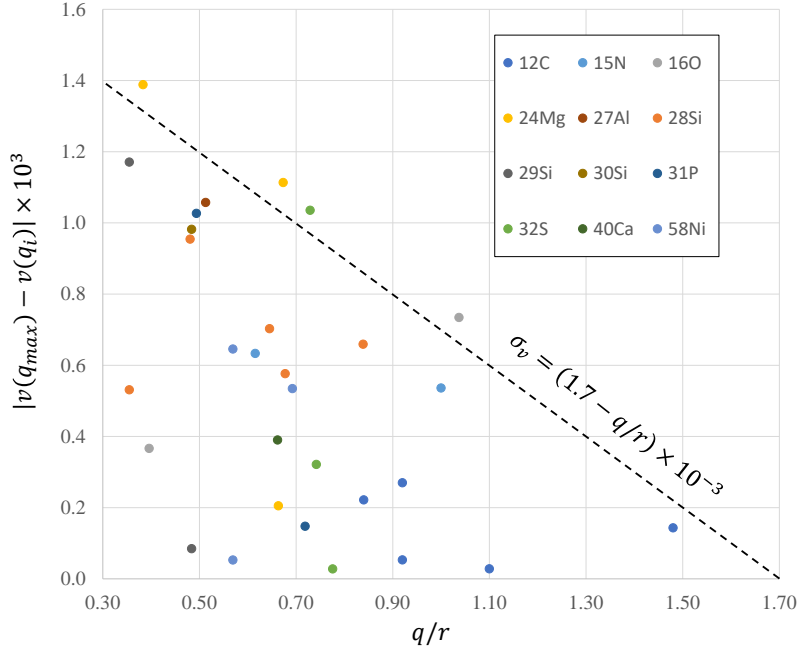


**Fig. 2:** Estimation of uncertainty in  $v$  factors based on a comparison of results at lower-than-maximal momentum transfer.

sub percent accuracy must include a discussion of the nuclear shape. Following Ref. [13], we note that in scattering experiments, a high momentum transfer (measured e.g. in  $\text{fm}^{-1}$ ) compared to the nuclear size is needed in order to be sensitive to higher moments of the charge distribution. Thus, the maximal momentum transfer over the RMS radius,  $q/r$ , is indicative of the ability of a scattering experiment to resolve subtle features of the charge distribution. For each nucleus on which electrons were scattered upon, we estimate the most probable value of  $v$  from the charge distribution obtained by the scattering experiments with the highest maximal  $q$ . These data are usually the ones in which a (nearly) model-independent analysis of the scattering data was done. The results are given in Tab. 1.

Having chosen the most probable value,  $v(q_{\text{max}})$ , we turn to bootstrap its uncertainty. To do that, for each nucleus in which one or more measurements with large  $q$  are available, we extract the less accurate factors  $v(q_i)$ 's from the rest of the scattering experiments whose parametrizations are given in Ref. [4, 12, 14]. We then look at the deviation  $|v(q_i) - v(q_{\text{max}})|$ , shown in Fig. 2. It is clearly seen that the lower the figure of merit  $q/r$ , the higher the chance the  $v$  factors will deviate much from their most probable values. In several cases, the deviation is unreasonably low, which we ascribe to a correlations in their analysis. These are difficult disentangle due to the partiality of the published information. In light of this we parameterise the uncertainty taking into account the most deviating points. To account for these possible deviations, we choose a simple uncertainty parametrization

$$\sigma_v(q, r) = (1.7 - q/r) \times 10^{-3}, \quad (3)$$

as shown in Fig. 2. The most sensitive scattering experiment, was in  $^{12}\text{C}$ , reaching  $q = 4.0 \text{ fm}^{-1}$  so that  $q/r = 1.6 \text{ fm}^{-2}$  and so, according to Eq. 3,  $\sigma_v = 10^{-4}$ . However, the majority of experiments are in the range  $q/r = 0.5 - 0.9 \text{ fm}^{-2}$  resulting in  $\sigma_v \sim 10^{-3}$ . For some nuclei relevant to this work no reliable scattering experiments are available. We estimate their  $v$  factors by interpolating from the neighbouring elements as shown in Fig. 3. Generous uncertainties are given for these interpolated values.

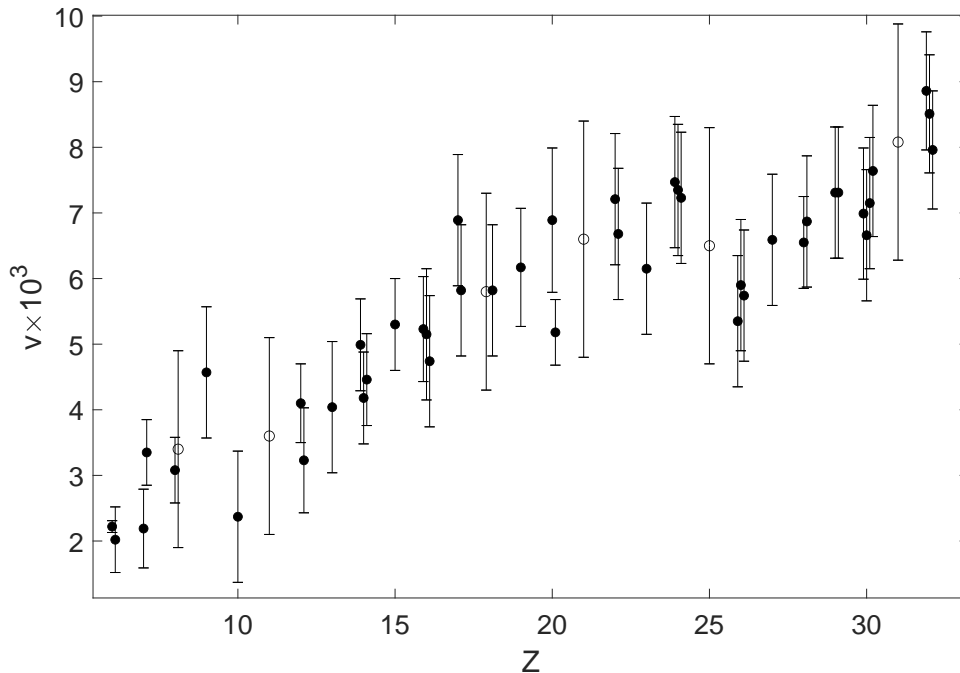


**Fig. 3:** Recommended  $v$  factors, with uncertainty estimated using Eq. 3. Open symbols denote interpolated values. Small horizontal shifts were introduced for clarity.

## 2.2. Reference radii

Employing Eq. 2, the  $v$  factors given in Tab. 1, and the BERs collected in [1], we compile a list of reference radii, given in Tab. 2. For the light nuclei  ${}^6\text{Li}$ ,  ${}^9\text{Be}$ ,  ${}^{11}\text{B}$ ,  ${}^{15}\text{N}$ , as well as the medium mass Cl isotopes, radii are not sufficiently well measured by muonic x-ray spectroscopy. We thus use values from scattering experiments (see also discussion in Ref. [5]). For each nucleus whose radius is extracted from muonic x-ray experiments, three distinct uncertainty contributions are taken into account. The first is related to the ‘pure’ experimental one, which stems from the statistical precision and calibration accuracy in the measured energies of the relevant transitions. The second is related to the uncertainty in the nuclear polarization correction as given in [1]. The third uncertainty is directly from that in the  $v$  factors. The different fractional uncertainty contributions are plotted in Fig. 4. From the figure we readily see that from carbon to Neon, experimental uncertainties dominate. From phosphorous onward, it is the charge-distribution uncertainty, unaccounted-for in prior compilations, is dominant. The trend continues, so that even larger missing uncertainties are expected for the heavier nuclei, as was recently pointed out [15].

We also plot in Fig. 4 the total fractional uncertainties given in the latest compilation [8]. As expected, they roughly follow the nuclear polarization trend above  $Z = 10$ , thus emphasizing the need for accounting for  $\sigma_{\text{CD}}$ , which are up to 4 times larger. Adopting the values in [8] would result in shifts of on average one of their reported uncertainty. This illustrates that the impact of the choice of the calibration factors in tab. 1, and demonstrates the importance of the increased uncertainty budget. It is worth noting that  $r({}^{12}\text{C})$  quoted in [8] lies 6 standard deviations away from our recommended value, which is taken from [16]. This might be due to a propagation of a typo in the uncertainty the Barret radii of carbon isotopes given in [17].

Having decided on the reference radii, we combine them with isotopic differences  $\delta r$  (or  $\delta r^2$ ) to obtain radii of all

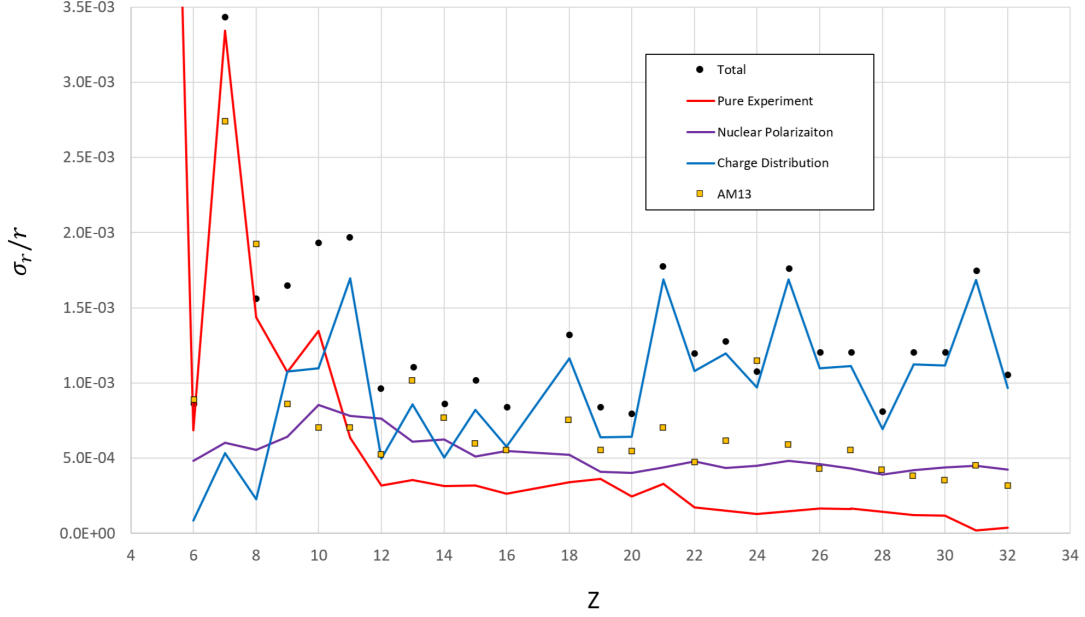


**Fig. 4:** Contributions to the uncertainty of reference radii as determined from muonic x-ray measurements. For each element, the numbers correspond to the isotope whose radius is best known. The open markers denote the corresponding total uncertainties given in [8].

measured isotopes of an element. The differences are mostly extracted from isotope shift measurements (reviewed e.g. in [18]) combined with theory calculations (see e.g. [19]). The subset of radii relevant to mirror nuclei is given in table 5, in which references to the isotope shift measurements and atomic theory literature can be found.

For a small set of the mirror nuclei, both the radius of the proton-rich and of the neutron-rich partner has been measured. Their difference is used below to make the mirror fit. Before that, we digress to improve the extraction of the radii of the neon chain, which plays a key role in the fit.

### 3. Re-calibration of the neon chain

Being a light element in which optical isotope shifts for several proton-rich isotopes were measured [20, 21], the neon chain plays a key role in this work. We now show that incorporating a recent novel measurement of the bound-electron g-factor isotope shift in hydrogen-like neon significantly improves the radii of the entire chain, which harbors important proton-rich isotopes taking part in the mirror fit.

First, we comment on the reference radius of the  $^{20}\text{Ne}$  nucleus. It is given in Tab. 2 as  $r_{20} = 3.001(6)$  fm. Its uncertainty is mostly from experiment, and with equal contributions from nuclear polarization, and charge distribution parametrization. It is also in agreement with  $r_{20} = 3.006(5)$  fm from Ref. [22], which is estimated from the corresponding BER using a two-parameter Fermi distribution with surface thickness  $t = 2.3$  fm. We estimated the uncertainty by changing  $t$  by 10%, while keeping  $r_{20} \sim 3.0$  fm and recording the variation in  $v$ . Another radius can be found in a recent compilation  $r_{20} = 3.0055(21)$  fm [8], with uncertainty smaller than the quadratic sum of experimental and nuclear polarization uncertainties. This is an example of how aggressive the uncertainties quoted in [8] are. It is worth noting that we estimate a smaller radius than the others. The reason for this is that we calculated the calibration factor  $v = 2.4(1.1)$  from the three Fermi distribution parameters given in [12] (Denoted by Ref. “Be85”), due to the relatively

high  $q_{eff} = 1.8 \text{ fm}^{-1}$  range covered. Adopting the charge distributions from either [23] or [24], which only extend to  $q_{eff} = 1 \text{ fm}^{-1}$ , results in  $v \sim 5$  giving  $r_{20} = 3.009 \text{ fm}$ . The 0.3% difference in the radius obtained using  $v$ -factors from different scattering experiments is a testament to the importance of accounting for uncertainty in the charge distribution. The lack of high momentum transfer scattering data in  $^{22}\text{Ne}$  prevents us from estimating its radius directly from its Barrett radius given in [22]. Assuming  $v_{22} = v_{20} \pm 0.5$ , in line with the isotopic variations from Tab. 1, returns a difference

$$\delta r_{20,22}^2 = -0.310(16)_{\text{exp}}(5)_{\text{NP}}(9)_{\text{v}} \text{ fm}^2, \quad (4)$$

where we observe that the uncertainty from a possible variation of the charge distribution between the isotopes is not negligible.

Optical isotope shifts were measured for the 614 nm transition in a long chain of neon isotopes [20, 21]. To calibrate the radii of the neon chain, a partial king plot procedure is used. It relies on the IS equation

$$\delta v_i^{A,A'} \approx K_i \mu^{A,A'} + F_i (\delta r^2)^{A,A'}, \quad (5)$$

with  $F_{614}$  calculated via many-body atomic theory and one differential radii pair to determine  $K_{614}$ . The resulting  $K_{614}$  and calculated  $F_{614}$  are then used to extract  $\delta r^2$  from optical isotope shifts. Originally,  $F_{614} = -40(4) \text{ MHz/fm}^2$  was estimated semi-empirically using the Goudsmit-Fermi-Segre method (GFS) [20]. Resulting in the radii of the chain that were limited by  $\sigma_F$ . A later *ab initio* calculation returned  $F_{614} = -30.5(1.5) \text{ MHz/fm}^2$  [25], where we adopted here the more conservative uncertainty estimate given in [26]. The disagreement between the semi-empirical and *ab initio* methods is attributed to the limited accuracy of the GFS formula, as discussed e.g. in [25, 27–29]. Using this  $F_{614}$ , the radii of the chain could be improved by up to a factor of 1.6 [25], with their uncertainty dominated by that of  $\delta r_{20,22}^2$  given in Eq. 4. It is thus clear that a better determination of  $\delta r_{20,22}^2$  would increase the accuracy far from stability.

Luckily, a new method has recently emerged to determine differential radii in even-even isotopes. This is accomplished through measuring the differences in the  $g$ -factors of single electron bounds to bare nuclei. For neon, such a measurement returned  $r_{20} - r_{22} = -0.0533(4) \text{ fm}$  corresponding to  $\delta r_{20,22}^2 = -0.3171(24) \text{ fm}^2$  [30]. A remarkable improvement by factor 8 over the value given in Eq. 4. Applying Eq. 5 with the highly accurate  $\delta r_{20,22}^2$  from the  $g$ -factor measurement results in improved differential radii of the entire neon chain. They are given in table 3. These are more precise by up to a factor 2.5 as compared with [25]. The improvement was somewhat curtailed by our more conservative uncertainty estimation for  $r_{20}$  and  $F_{614}$ . The current uncertainty budget both motivates new optical measurements with higher precision, and a more accurate calculation of  $F_{614}$ .

This example shows the tremendous impact of measuring a single  $\delta g_{\text{bound}}$ , and motivates extending such measurements to other stable even-even pairs.

#### 4. The mirror shift fit

Extensive *ab initio* calculations suggest that the differences in radii between mirror nuclei (mirror shifts) are proportional to the isospin asymmetry  $I = (N - Z)/A$ , at least up to  $I \approx 0.2$  [31]. The experimental situation is not as healthy. In contrast with isotope shifts, which can be measured directly via optical spectroscopy, mirror shifts are difficult to measure with high fractional precision. To obtain them, one has to take the difference between the absolute radii of the mirror pair, contending with large experimental and theoretical uncertainties, which are emphasized in the

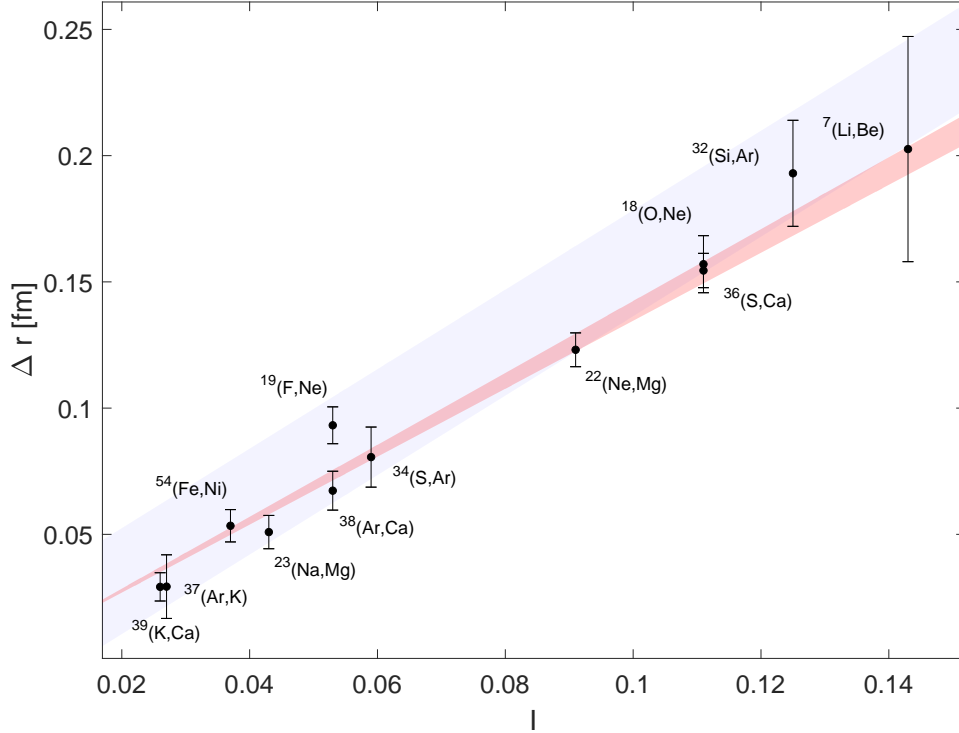


**Fig. 5:** Linear fit to the mirror shift. Data-points are the individual shifts from Tab. 4. The dark shaded region is the 68% confidence interval of the fitted slope given in Eq. 6. The light shaded region is the 68% confidence interval calculated from first principles [31].

previous sections. Nevertheless, with the reference radii given in Table 2,  $\delta r^2$  from the literature (the references are given in Table 5), and the re-calibrated neon differential radii given in Table 3, we have all the ingredients to test the linear theoretical prediction experimentally.

The relevant data is given in Table 4. We excluded the pair  $^{21}\text{Na}$ - $^{21}\text{Ne}$ , as its uncertainty is too large to be of use. We also did not include the pairs with Cl isotopes, as their radii were determined from electron scattering experiments which are of limited reliability. The result of a one parameter analytical fit to the weighted mirror shifts is shown in Figure 5. It has a reduced Chi-square of  $11.5/11 = 1.04$  indicating that a such a fit is not inconsistent with the data. The resulting mirror shift parametrization is

$$\Delta_I = r_{N,Z}(I) - r_{Z,N}(I) = 1.382(34) \times I \text{ fm.} \quad (6)$$

The structure of this work enables to remove certain ingredients from the analysis to test their effect. We find that nearly half of the uncertainty given in Eq. 6 stems from that of the charge distributions, previously overlooked in the literature. Omitting it would result in a reduced  $\chi^2$  of 2.3. The second-largest contributor is the uncertainty in the differential radii, as extracted from optical isotope shift measurements. It originates mostly from the atomic factors and not the statistical accuracy of the optical measurements (see e.g. [32]).

The empirically determined slope of Eq. 8, agrees with the band spanning nuclear theory calculations  $\Delta_I = (1.574 \times I) \pm 0.021 \text{ fm}$  [31], also shown in Figure 5. To extend the comparison between experiment and theory, it would thus be very interesting to add experimental data at high asymmetry  $0.12 < I$  for which no precise data is currently available. The pair which weight is the largest in the fit is  $^{36}\text{Ca}$ - $^{36}\text{S}$ , which combines high experimental accuracy with a large

asymmetry. The pair which sits the farthest from the fit, 2.3 standard errors away, is  $^{19}\text{F}$ – $^{19}\text{Ne}$ . Excluding it brings down the reduced  $\chi^2$  to 0.59. It could be a statistical deviation, an underestimated error in the radii determinations or a genuine nonlinearity.

Having validated that the mirror shift is indeed proportional to  $I$ , we can use the fit results of Eq. 6 to predict the unknown radii of mirror nuclei (colored in orange in Fig. 1) from their partners which radii are already known. The results are given in italics in Table 5, where the radii of 73 mirror partners are predicted. We note that their uncertainty is mostly dominated by that of the measured partner and not by the uncertainty in the mirror shift fit. This means that small deviations from linearity, such as that of the  $^{19}\text{F}$ – $^{19}\text{Ne}$  pair, have a mostly negligible effect on our predicted radii.

## 5. Example applications

### 5.1. Testing atomic many-body calculations

Optical isotope shift in Na have been measured a long time ago for a long chain of isotopes [33]. However, extracting  $\delta r^2$  from these measurements has been highly difficult. This is because Na is both mono-isotopic, preventing muonic x-ray measurement in more than the stable isotope, and light - making the accuracy goal in its mass shift factor calculation highly challenging.

Specifically, recent calculation of the IS factors of Na, combined with isotope shift measurements, returns  $r_{21} = 2.97(1)[6]$  fm with uncertainty dominated by that of the mass shift factor calculation. This value is not accurate enough to be useful in the mirror fit. However, we can inverse this logic and use the fit results of Eq. 6 to get  $r_{21} = 3.029(7)$  fm which agrees with the literature value but enjoys an uncertainty smaller by an order of magnitude. Combining the reference radius  $r_{23} = 2.992(6)$  fm from table 2 returns the MS difference  $\delta r_{23,21}^2 = 0.22(5)$  fm<sup>2</sup>. It is much more accurate, and in agreement with  $\delta r_{23,21}^2 = -0.13(5)[34]$  fm<sup>2</sup> given in [34].

Armed with one MS radius difference in the Na chain, we can now calibrate its entirety using the calculated FS factor, which is considered reliable [34]. Employing Eq. 5 with  $\delta r_{23,21}^2 = 0.22(5)$  fm<sup>2</sup> and  $F = -39.3(3)$  MHz/fm<sup>2</sup> returns  $K_{D1} = 384.7(6)$  GHz u, with uncertainty equally from experiment and  $\delta r_{23,21}^2$ . The extracted radii of the chain based on these values, along with their mirror partner values, are given in table 5. This MS factor agrees with, and is more accurate than, that which is calculated with relativistic coupled cluster method  $K_{D1} = 388(3)$  GHz u [34]. It thus sets a benchmark for the next generation calculations [19]. The mass shift also agrees with a semi-empirical estimation based on a combination of matter radii and calculated neutron skins  $K_{D1} = 384.0(1.3)$  [34].

### 5.2. Charge and weak radii of CKM-determining isotopes

The largest CKM matrix element  $V_{ud}$ , which uncertainty dominates that of the top row unitarity test, is extracted from measured parameters (half-lives, Q-values, etc.) in superallowed  $0^+ \rightarrow 0^+$  beta transitions between states with isospin  $T = 1$ . It is usually parameterized as

$$V_{ud}^{-2} \propto ft(1 + \delta'_R)(1 + \delta_{NS} - \delta_C)(1 + \Delta_R^V), \quad (7)$$

with  $f(Q)$  the statistical rate function,  $t$  the beta decay half-life,  $\Delta_R^V$  is a nucleus-independent (universal) correction, and  $\delta_i$  are various nucleus-dependant corrections; their uncertainty now dominates that of the currently accepted value of  $V_{ud}$  [35].

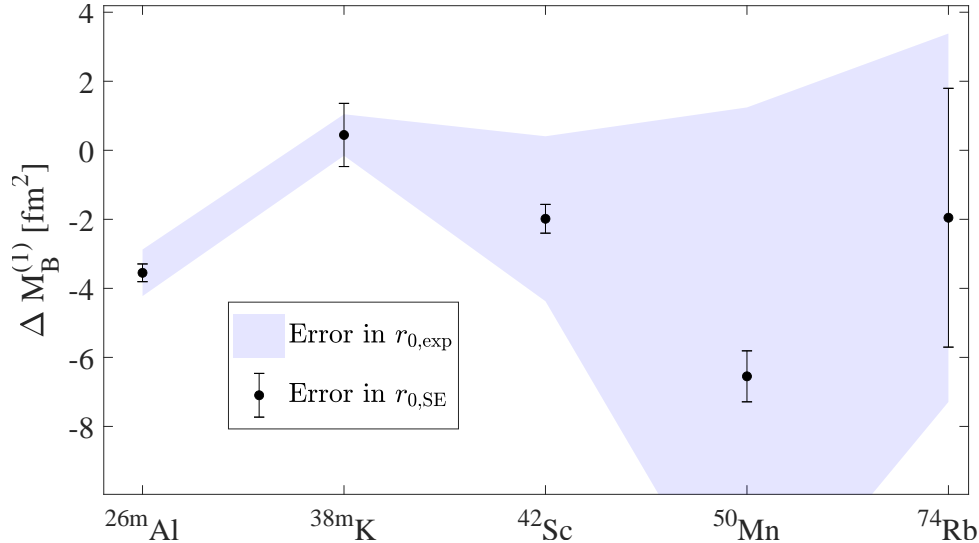


**Fig. 6:** Testing for isospin symmetry breaking by comparing measured (exp) and semi-empirical (SE) radii. See Eq. 10 and Table 7.

Recently, the role of nuclear charge radii in calculating  $f$  has been put to the spotlight [36], pointing that their role, and the effect in their uncertainty is much larger than previously considered. Moreover, it has been recognized that radii may constrain the isospin symmetry breaking correction  $\delta_C$  as well [37]. Work on a fully data-driven analysis of the  $ft$ -values of superallowed decays has pointed the need to complete the determinations of charge radii of all members of each isotriplet [36].

Here, the empirical mirror relation, already gives rise to reliable radii estimation of all nuclei with  $T_z = -1$  which are involved in the determination of  $V_{ud}$  (see table 5). However, some  $T_z = 0$  nuclei play a key role as well [35], with only a handful of their radii measured. To estimate the radii of these nuclei, we first denote the radii of triplet nuclei by  $r_{T_z}$  with  $T_z = -1, 0, +1$ . The mirror then fit directly gives

$$r_{-1}^2 - r_{+1}^2 = \Delta_I(2r_{+1} + \Delta_I) \quad (8)$$

with  $\Delta_I$  given in Eq. 6. This form is suitable for combining with equation 16 from [38], to obtain a semiempirical isotriplet interpolation formula for the radius of  $T_z = 0$  nuclei

$$r_{0,\text{SE}}^2 = r_{+1}^2 + \frac{Z_{-1}}{2Z_0} \Delta_I(2r_{+1} + \Delta_I). \quad (9)$$

Using Eq. 9, can determine the radii of  $T_z = 0$  nuclei directly, they are given in Tab. 7. Their uncertainty spans 0.1 – 1.5% and is dominated by that of  $r_{+1}$ . The least well-known triplet is that with  $A = 10$ , motivating an improved determination of the radius of  $^{10}\text{Be}$ .

If all else is under control, and spin-orbit corrections within a triplet are neglected, then the difference between experimental and semi-empirical radii can help to search for, or constrain, isospin-symmetry-breaking (ISB) within the isotriplets. Plugging Eq. 9 to Eq. 10 from Ref. [37] we obtain the compact expression

$$\Delta M_B^{(1)} = Z_0(r_{0,\text{SE}}^2 - r_{0,\text{exp}}^2), \quad (10)$$

which vanishes in the isospin-symmetric limit. The results are given in Table 7, and plotted in Fig. 6. The most stringent constraint on ISB is with the  $A = 38$  triplet, for which  $|\Delta M_B^{(1)}(38)| \leq 1.5 \text{ fm}^2$ , comparing well with theoretical

predictions, which are as high as  $|\Delta M_B^{(1)}(38, \text{DFT})| \leq 0.42 \text{ fm}^2$  [37]. For the  $A = 26$  triplet, one may conclude that ISB effects indeed contribute at the level  $\Delta M_B^{(1)}(26) = -3.4(0.7) \text{ fm}^2$ . However, the magnitude of the largest calculated effect is much smaller, at  $\Delta M_B^{(1)}(26, \text{DFT}) = -0.12 \text{ fm}^2$  [37]. The dominating uncertainty in  $\Delta M_B^{(1)}(26)$  can be traced back to challenging atomic many-body calculations of the mass-shift factor needed in order to interpret optical isotope shifts measurements. This factor is calculated in Ref. [39], quoting 2% uncertainty. Such an uncertainty might be considered aggressive if one takes into account the deviations found in similar calculations for Zn I [40]. A state-of-the-art calculation was recently reported [41], which confirmed the previous one and reduced the uncertainty.

Further scrutiny is advised before drawing any conclusion about the existence of large ISB corrections: 1. Measuring isotope shifts in more transitions and testing the the same MS radius difference is extracted from each (see e.g. [42]). 2. Performing more independent calculations with different methods [19]). 3. Measuring  $r(^{26}\text{Al})$  directly with muonic atom x-ray spectroscopy of a microgram-scale target [43], and then extract  $r(^{26m}\text{Al})$  from the isomer shift which is largely independent of the most difficult part of the many-body atomic theory calculation.

We now turn to estimating the weak radius of the triplets, which is of interest e.g. for calculating recoil corrections involved in extracting the  $V_{ud}$  matrix element [38]. Combining Eq. 8 and Eq. 16 in [38], we obtain another simple formula

$$r_{\text{CW}}^2 = r_{+1}^2 + \frac{Z-1}{2} \Delta_I (2r_{+1} + \Delta_I), \quad (11)$$

which connects weak radii with the well measured ones of  $r_{+1}$  and the result of the mirror fit  $\Delta_I$ . We note that the role of  $\Delta_I$  in Eq. 11 is larger, by a factor  $Z_0$  than its role in Eq. 9. Correspondingly, the weak radii calculated via Eq. 11 and given in Tab. 7, have an uncertainty mostly dominated by that of  $\Delta_I$ , and not  $r_{+1}$ . This means that the key to improving  $r_{\text{CW}}^2$  for most isotriplets is in reducing the error in the mirror slope  $\Delta_I$ . The notable exception is the  $A = 10$  triplet which would also benefit from a more accurate measurement of  $r(^{10}\text{Be})$ . We also quote in Tab. 7 the  $R_{\text{CW}}^2$  from Ref. [38], only available for half of the cases of interest. For the known cases we reduced the uncertainty by, on average, a factor of 13. A notable difference in  $R_{\text{CW}}^2$ , by 2.4 standard deviations, is seen for the  $A = 18$ . It stems from missing uncertainties in the tabulation of Ref. [8], and from the shifted field shift factor as discussed in section 3.

## 6. Summary

In this work we reanalyzed the absolute root-mean-square charge radii of stable nuclei up to  $Z = 32$ . Admittedly, we have used the traditional ‘Barret moment’ recipe for combined analysis of muonic x rays and electron scattering. We showed that even within this simplified framework, there is a notably large missing uncertainty contribution from our knowledge of the charge distribution. It is our aim for this analysis to trigger a modern extraction of charge radii from muonic atom data, with renewed calculations of nuclear polarization, nuclear model, QED corrections, accounting for deformation, hyperfine structure, etc.

The reference radii are combined with isotopic differences, stemming from measured electronic isotope shifts and atomic theory calculations, to obtain those of isotopic chains. In some cases, large uncertainties in the theory have not been taken into account, which is remedied here. Further emphasis is put into the neon chain which is recalibrated using a novel measurement in coupled highly charged ions [30]. The physics discussed in this work would greatly benefit from extending such measurements to more even-even pairs, especially of Si, Ar, and Ca.

Having constructed the database, we focus on 12 pairs of mirror nuclei with reasonably measured radii. Their difference is found to be proportional to the isospin asymmetry, confirming the calculations of [31], at least for nuclei with  $18 < A$  and  $I < 0.12$ . From the fitted proportionality constant and its uncertainty, the radii of 73 previously unknown mirror partners are predicted.

Two example of applications benefiting from these new or improved radii are given. First, we use the predicted radius of  $^{21}\text{Na}$  with the calculated field shift factor of a relevant transition to determine its mass shift factor. This factor is used to recalibrate the radii of the chain spanning  $^{20}\text{Na}$  to  $^{31}\text{Na}$ , also giving the radii of their mirror partners, such as  $^{20}\text{F}$ . The factor also compares favourably with atomic many-body calculations [34], setting a stringent benchmark for the next generation of calculation methods [19].

The second example deals with radii of isotriplet nuclei as sandbox for isospin symmetry breaking studies. Assuming that symmetry breaking is negligible as compared with the relevant uncertainties. In this case, we can combine the fit result with the relation from [38] to obtain a simple equation for determining unknown radii of  $T = 1, T_z = 0$  nuclei from the mostly well known radii of those with  $T = 1, T_z = 1$ . This completes a model-independent, high-precision extraction of the charge radii of all nuclei involved in the testing of the unitarity of the CKM matrix.

Relaxing the assumption of zero isospin symmetry breaking effects enables to test it. Without the mirror fit, this could only be done with the  $A = 38$  triplet. Here, four more cases are considered. We find a general agreement except for with the  $A = 26$  case. This calls for refined isotope shift measurements in the Aluminum chain, more atomic factor calculations of the relevant transitions, and a direct measurement of the radioactive  $^{26}\text{Al}$  radius with muonic atoms and microgram targets. Extending recent measurements from neutron- to proton-rich Si would be beneficial as well.

Finally, we extract the weak radii of all nuclei involved in the testing of the unitarity of the CKM matrix. Half of these weak radii were previously unknown, and rest are improved by an order of magnitude.

## Acknowledgement

We thank CY Seng, M Gorshteyn and M Heines their insightful comments. The support of the Council for Higher Education Program for Hiring Outstanding Faculty Members in Quantum Science and Technology is acknowledged.

**Table 1**

$v$  factors of reference nuclei for which high- $q$  scattering measurements are available. They are calculated from the charge distributions whose model is given in the ‘model’ column and on which information can be found in the reference of the ‘Ref.’ column. The uncertainty  $\sigma_v$  is calculated from Eq. 3 with  $q_{\max}r$ . The  $v$  factors of elements in which no scattering results are available, we interpolated, as indicated by ‘Int.’ in the ‘Model’ column, with large uncertainties (see Fig. 3).

el.	Z	A	$v \times 10^3$	$\sigma_v$	Model	Ref.	$q_{\max} \text{ fm}^{-1}$	$q_{\max}r$
C	6	12	2.2	0.1	FB	VJV Ca80	4.0	1.6
N	7	14	2.2	0.5	3pF	VJV La82	2.9	1.2
	7	15	3.3	0.5	FB	Fri Vr88	3.2	1.2
O	8	16	3.1	0.2	SOG	VJV Si70b	4.0	1.5
F	9	19	4.6	1.1	2pF	VJV Oy75	1.8	0.6
Ne	10	20	2.4	1.1	3pF	VJV Be85	1.8	0.6
Na	11	23	3.6	1.5	Int.			
Mg	12	24	4.1	0.5	SOG	VJV Li74	3.6	1.2
	12	26	3.2	0.7	FB	Fri So88	3.0	1.0
Al	13	27	4.0	0.9	FB	VJV Ro86	2.6	0.8
Si	14	28	5.0	0.5	SOG	VJV Li74	3.7	1.2
	14	29	4.2	0.9	FB	VJV Mi82	2.6	0.8
	14	30	4.5	0.7	FB	[14]	3.0	1.0
P	15	31	5.3	0.8	FB	[14]	2.8	0.9
S	16	32	5.2	0.6	FB	[14]	3.7	1.1
	16	34	5.1	0.9	FB	[44]	2.6	0.8
	16	36	4.7	0.9	FB	[44]	2.6	0.8
Cl	17	35	6.9	1.2	3pF	Br80	1.7	0.5
	17	37	5.8	1.2	3pF	Br80	1.7	0.5
Ar	18	38	5.8	1.7	Int.			
	18	40	5.8	1.2	FB	VJV Ot82	1.8	0.5
K	19	39	6.2	0.6	SOG	VJV Li74	3.6	1.1
Ca	20	40	6.9	0.6	SOG	VJV Si79	3.7	1.1
	20	48	5.2	0.7	SOG	VJV Si74	3.4	1.0
Sc	21	45	6.6	1.7	Int.			
Ti	22	48	7.2	1.1	FB	VJV Se85	2.2	0.6
	22	50	6.7	1.1	FB	VJV Se85	2.2	0.6
V	23	51	6.2	1.2	2PF	VJV Pe73	1.8	0.5
Cr	24	50	7.5	1.0	FB	VJV Li83c	2.6	0.7
	24	52	7.4	1.0	FB	VJV Li83c	2.6	0.7
	24	54	7.2	1.0	FB	VJV Li83c	2.6	0.7
Mn	25	55	6.5	1.7	Int.			
Fe	26	54	5.3	1.1	FB	VJV Wo76	2.2	0.6
	26	56	5.9	1.1	FB	VJV Wo76	2.2	0.6
	26	58	5.7	1.1	FB	VJV Wo76	2.2	0.6
Co	27	59	6.6	1.1	FB	VJV Sc77	2.2	0.6
Ni	28	58	6.6	0.7	SOG	VJV Ca80b	3.9	1.0

**Table 1**

$v$  factors of reference nuclei for which high- $q$  scattering measurements are available. They are calculated from the charge distributions whose model is given in the ‘model’ column and on which information can be found in the reference of the ‘Ref.’ column. The uncertainty  $\sigma_v$  is calculated from Eq. 3 with  $q_{\max}r$ . The  $v$  factors of elements in which no scattering results are available, we interpolated, as indicated by ‘Int.’ in the ‘Model’ column, with large uncertainties (see Fig. 3).

el.	Z	A	$v \times 10^3$	$\sigma_v$	Model	Ref.	$q_{\max} \text{ fm}^{-1}$	$q_{\max}r$
Cu	29	63	7.3	1.1	FB	VJV Sc77	2.2	0.6
	29	65	7.3	1.1	FB	VJV Sc77	2.2	0.6
Zn	30	64	7.0	1.1	FB	WO76	2.2	0.6
	30	66	6.7	1.1	FB	WO76	2.2	0.6
	30	68	7.1	1.1	FB	WO76	2.2	0.6
	30	70	7.6	1.1	FB	WO76	2.2	0.6
	31	71	8.1	1.7	Int.			
Ge	32	70	8.9	1.0	FB	Ma84	2.9	0.7
	32	72	8.5	1.0	FB	Ma84	2.9	0.7
	32	74	8.0	1.0	FB	Ma84	2.9	0.7

**Table 2**

Reference radii used in this work. Unless stated otherwise in the note, they are determined via Eq. 1 and 2 with the  $2P_{3/2} - 1S$  Barret radii given in [1] and the  $\nu$  factors from tab. 1. Uncertainties are denoted by  $\sigma$  and correspond to statistics and energy calibration (exp), nuclear polarization (NP), and charge distribution (CD) as resulting from the  $\nu$  factors of Tab. 1

el.	Z	A	$r_{\text{ch}}$	$\sigma_{\text{exp}}$	$\sigma_{\text{NP}}$	$\sigma_{\text{CD}}$	$\sigma_{\text{tot}}$	Note
Li	3	6	2.589	0.039			0.039	A
Be	4	9	2.519	0.012		0.030	0.032	B
B	5	11	2.411	0.021			0.021	C
C	6	12	2.483	0.002	0.001	0.000	0.002	D
N	7	14	2.556	0.009	0.002	0.001	0.009	
	7	15	2.612	0.009			0.009	E
O	8	16	2.701	0.004	0.001	0.001	0.004	F
F	9	19	2.902	0.003	0.002	0.003	0.005	†
Ne	10	20	3.001	0.004	0.003	0.003	0.006	†
Na	11	23	2.992	0.002	0.002	0.005	0.006	†
Mg	12	24	3.056	0.001	0.002	0.002	0.003	†
	12	26	3.030	0.001	0.002	0.002	0.003	†
Al	13	27	3.061	0.001	0.002	0.003	0.003	†G
Si	14	28	3.123	0.001	0.002	0.002	0.003	†
P	15	31	3.190	0.001	0.002	0.002	0.003	
S	16	32	3.262	0.001	0.002	0.003	0.003	
	16	34	3.284	0.001	0.002	0.003	0.004	
	16	36	3.298	0.001	0.001	0.003	0.004	
Cl	17	35	3.388	0.015			0.015	H
Cl	17	37	3.384	0.015			0.015	H
Ar	18	38	3.402	0.002	0.003	0.005	0.006	
	18	40	3.427	0.001	0.002	0.003	0.004	
K	19	39	3.435	0.001	0.001	0.003	0.004	
Ca	20	40	3.481	0.001	0.001	0.004	0.004	
	20	48	3.475	0.001	0.001	0.002	0.002	
Sc	21	45	3.548	0.001	0.002	0.006	0.007	
Ti	22	48	3.595	0.001	0.002	0.004	0.004	
	22	50	3.572	0.001	0.002	0.004	0.004	
V	23	51	3.598	0.001	0.002	0.004	0.004	
Cr	24	50	3.664	0.000	0.002	0.004	0.004	
	24	52	3.644	0.000	0.002	0.004	0.004	
	24	54	3.689	0.001	0.002	0.004	0.004	
Mn	25	55	3.705	0.001	0.002	0.007	0.007	
Fe	26	54	3.688	0.001	0.002	0.004	0.004	I
	26	56	3.733	0.001	0.002	0.004	0.004	I
Co	27	59	3.786	0.001	0.002	0.004	0.004	
Ni	28	58	3.773	0.001	0.001	0.003	0.003	J
Cu	29	65	3.902	0.0005	0.001	0.004	0.004	

**Table 2**

Reference radii used in this work. Unless stated otherwise in the note, they are determined via Eq. 1 and 2 with the  $2P_{3/2} - 1S$  Barret radii given in [1] and the  $\nu$  factors from tab. 1. Uncertainties are denoted by  $\sigma$  and correspond to statistics and energy calibration (exp), nuclear polarization (NP), and charge distribution (CD) as resulting from the  $\nu$  factors of Tab. 1

el.	Z	A	$r_{\text{ch}}$	$\sigma_{\text{exp}}$	$\sigma_{\text{NP}}$	$\sigma_{\text{CD}}$	$\sigma_{\text{tot}}$	Note
Zn	30	68	3.964	0.0005	0.002	0.004	0.004	K
Ga	31	71	4.014	0.0001	0.001	0.007	0.007	
Ge	32	72	4.059	0.0002	0.002	0.004	0.004	

- A. Estimated through a recent (nearly) model-independent combined analysis of several electron scattering experiments [45]  
B. Estimated from a model-dependent analysis of an electron scattering experiment covering a narrow momentum transfer range [46]. The same publication quotes a radius for  $^{12}\text{C}$  which deviates by 3 standard errors from its modern value. We added a systematic uncertainty to account for this deviation.  
C. Calculated from the difference  $r(^{12}\text{C}) - r(^{11}\text{B}) = 0.072(21)$  fm measured via elastic pion scattering [47]  
D. Extracted from a combined analysis of high resolution muonic x-ray measurements and electron scattering experiments going beyond the Barret moment recipe [16, 48]. This radius agrees with the dispersion-corrected radius from electron scattering [49]  
E. Based on electron scattering over a wide momentum transfer range [50]. Dispersion corrections are not included  
F. Notice that the statistical uncertainty in the Barret moment given in [51] is overestimated due to a typo  
G. An identical radius appears in [9], with a more conservative uncertainty estimate stemming from the charge distribution  
H. Muonic x-rays were only measured with a naturally-abundant sample [52]. Radii deduced from electron scattering experiment [53]. Missing uncertainty due to model dependence.  
I. A different combined analysis method, in which the uncertainties in the electron scattering experiment are accounted for, gives  $r_{54} = 3.692(5)$  fm and  $r_{56} = 3.737(5)$  fm [54] after scaling to the modern values of the Barret equivalent radii.  
J. A different combined analysis method, in which the uncertainties in the electron scattering experiment are accounted for, gives  $r_{58} = 3.774(5)$  fm [54] after scaling to the modern value of the Barret equivalent radius.  
K. A different combined analysis method, in which the uncertainties in the electron scattering experiment are accounted for, gives  $r_{68} = 3.966(5)$  fm [54] after scaling to the modern value of the Barret equivalent radius.  
† The experimental uncertainty in Fricke’s book is only statistical. To obtain the full uncertainty the original publication must be consulted.

**Table 3**

Re-calibrated radii of the Neon chain, whose optical isotope shifts are given in [21], using  $r_{20} - r_{22} = 0.0533(4)$  fm [30],  $F_{214} = -30.5(1.5)$  MHz/fm<sup>2</sup> [25, 26], and  $r_{20} = 3.001(6)$  fm from Tab. 2.

A	$\delta r_{20,A}^2$	$\sigma_{\text{stat}}$	$\sigma_{\text{K,F}}$	$\sigma_{\text{tot}}$	$r_A$	$\sigma_{\delta r^2}$	$\sigma_{r_{20}}$	$\sigma_{\text{tot}}$
17	0.082	0.038	0.030	0.049	3.015	0.008	0.006	0.010
18	-0.401	0.020	0.042	0.047	2.934	0.008	0.006	0.010
19	-0.038	0.024	0.012	0.027	2.995	0.005	0.006	0.007
20	0				3.001		0.006	0.006
21	-0.230	0.018	0.005	0.019	2.963	0.003	0.006	0.007
22	-0.317			0.002	2.948	0.000	0.006	0.006
23	-0.601	0.045	0.012	0.047	2.899	0.008	0.006	0.010
24	-0.634	0.025	0.011	0.027	2.894	0.005	0.006	0.008
25	-0.336	0.022	0.023	0.032	2.945	0.005	0.006	0.008
26	-0.374	0.023	0.028	0.036	2.938	0.006	0.006	0.009
28	0.006	0.046	0.056	0.073	3.002	0.012	0.006	0.013

**Table 4**

Input mirror shifts  $\Delta_I$  to the mirror fit, based on the reference radii of Table 2, with radii differences taken from the references given in Table 5

A	I	el.	Z	N	r fm	el.	Z	N	r fm	$\Delta_I$ fm	$\Delta_I/I$ fm	Weight fm <sup>-2</sup>	n $\sigma$
7	0.14	Li	3	4	2.449(41)	Be	4	3	2.646(33)	0.197(53)	1.42(37)	7	0.0
18	0.11	O	8	10	2.777(07)	Ne	10	8	2.934(09)	0.161(15)	1.45(13)	96	0.3
19	0.05	F	9	10	2.902(04)	Ne	10	9	2.995(06)	0.093(07)	1.77(14)	52	2.7
22	0.09	Ne	10	12	2.948(04)	Mg	12	10	3.071(05)	0.123(07)	1.35(07)	186	0.5
23	0.04	Na	11	12	2.992(05)	Mg	12	11	3.043(04)	0.051(07)	1.17(15)	43	1.4
32	0.13	Si	14	18	3.154(13)	Ar	18	14	3.346(17)	0.193(21)	1.54(17)	36	0.9
34	0.06	S	16	18	3.284(04)	Ar	18	16	3.365(11)	0.081(12)	1.37(20)	24	0.1
36	0.11	S	16	20	3.298(04)	Ca	20	16	3.452(06)	0.155(07)	1.39(06)	270	0.0
37	0.03	Ar	18	19	3.390(07)	K	19	18	3.419(10)	0.029(13)	1.09(47)	5	0.7
38	0.05	Ar	18	20	3.402(06)	Ca	20	18	3.469(04)	0.067(08)	1.28(15)	47	0.8
39	0.03	K	19	20	3.435(04)	Ca	20	19	3.464(04)	0.029(06)	1.14(22)	21	1.2
54	0.04	Fe	26	28	3.688(04)	Ni	28	26	3.741(05)	0.053(06)	1.44(17)	34	0.3

**Table 5**

Charge radii of mirror nuclei. Known radii are taken from Tab. 2 along with isotopic differences taken from the indicated references. Predicted radii relying on the validity of Eq. 6 are given in italics.

A	I	el.	Z	N	r	Ref./Note	el.	Z	N	r	Ref./Note
7	0.14	Be	4	3	2.646(33)	[55]	Li	3	4	2.449(41)	[56, 57]
8	0.25	B	5	3	<i>2.685(45)</i>		Li	3	5	2.339(44)	[45, 58]
9	0.33	C	6	3	<i>2.705(47)</i>		Li	3	6	2.245(46)	[45, 58]
10	0.20	C	6	4	<i>2.638(36)</i>		Be	4	6	2.361(36)	[55]
11	0.09	C	6	5	<i>2.536(21)</i>		B	5	6	2.411(21)	
13	0.08	N	7	6	<i>2.564(04)</i>		C	6	7	2.458(02)	[59]
14	0.14	O	8	6	<i>2.705(10)</i>		C	6	8	2.508(09)	[60] A
15	0.07	O	8	7	<i>2.704(09)</i>		N	7	8	2.612(09)	
17	0.06	F	9	8	<i>2.774(08)</i>		O	8	9	2.693(08)	[61] B
17	0.18	Ne	10	7	3.015(10)	Tab. 3	N	7	10	<i>2.771(12)</i>	
18	0.11	Ne	10	8	2.934(10)	Tab. 3	O	8	10	2.777(07)	[62] C
19	0.05	Ne	10	9	2.995(07)	Tab. 3	F	9	10	2.902(05)	
20	0.10	Na	11	9	<i>2.983(25)</i>	Tab. 6	F	9	11	<i>2.845(25)</i>	
21	0.05	Na	11	10	<i>3.029(07)</i>		Ne	10	11	2.963(07)	Tab. 3
21	0.14	Mg	12	9	3.067(07)	[34, 63]	F	9	12	<i>2.869(09)</i>	
22	0.09	Mg	12	10	3.071(05)	[34, 63]	Ne	10	12	2.948(06)	[30]
23	0.04	Mg	12	11	3.043(04)	[34, 63]	Na	11	12	2.992(06)	
23	0.13	Al	13	10	<i>3.080(11)</i>		Ne	10	13	2.899(10)	Tab. 3
24	0.08	Al	13	11	<i>3.078(11)</i>		Na	11	13	<i>2.963(11)</i>	Tab. 6
24	0.17	Si	14	10	<i>3.124(10)</i>		Ne	10	14	2.894(08)	Tab. 3
25	0.04	Al	13	12	<i>3.082(04)</i>		Mg	12	13	3.026(03)	[34, 63]
25	0.12	Si	14	11	<i>3.129(15)</i>		Na	11	14	<i>2.963(14)</i>	Tab. 6
26	0.08	Si	14	12	<i>3.136(04)</i>		Mg	12	14	3.030(03)	
26	0.15	P	15	11	<i>3.190(17)</i>		Na	11	15	<i>2.977(16)</i>	Tab. 6
27	0.04	Si	14	13	<i>3.111(04)</i>		Al	13	14	3.060(03)	
27	0.11	P	15	12	<i>3.181(05)</i>		Mg	12	15	3.027(03)	[34, 63]
27	0.19	S	16	11	<i>3.256(22)</i>		Na	11	16	<i>3.000(21)</i>	Tab. 6
28	0.07	P	15	13	<i>3.157(09)</i>		Al	13	15	3.058(09)	[9, 41]
28	0.14	S	16	12	<i>3.261(06)</i>		Mg	12	16	3.063(04)	[34, 63]
29	0.03	P	15	14	<i>3.165(06)</i>		Si	14	15	3.118(06)	[64]
29	0.10	S	16	13	<i>3.221(15)</i>		Al	13	16	3.078(15)	[9, 41]
30	0.07	S	16	14	<i>3.226(06)</i>		Si	14	16	3.134(05)	[64]
31	0.03	S	16	15	<i>3.235(03)</i>		P	15	16	3.190(03)	
31	0.16	Ar	18	13	<i>3.323(31)</i>		Al	13	18	3.099(31)	[9, 41]
32	0.13	Ar	18	14	3.346(17)	[65, 66] D	Si	14	18	3.154(13)	[64]
33	0.09	Ar	18	15	3.343(15)	[65, 66] D	P	15	18	<i>3.217(15)</i>	
34	0.06	Ar	18	16	3.365(11)	[65, 66] D	S	16	18	3.284(04)	
35	0.03	Ar	18	17	3.363(11)	[65, 66] D	Cl	17	18	<i>3.323(11)</i>	
36	0.06	K	19	17	3.406(14)	[67, 68]	Cl	17	19	<i>3.329(14)</i>	
36	0.11	Ca	20	16	3.452(06)	[69, 70]	S	16	20	3.298(04)	

**Table 5**

Charge radii of mirror nuclei. Known radii are taken from Tab. 2 along with isotopic differences taken from the indicated references. Predicted radii relying on the validity of Eq. 6 are given in italics.

A	I	el.	Z	N	$r$	Ref./Note	el.	Z	N	$r$	Ref./Note
37	0.03	K	19	18	3.419(10)	[67, 68]	Ar	18	19	3.390(07)	[66]
37	0.08	Ca	20	17	3.451(06)	[69, 70]	Cl	17	20	<i>3.338(07)</i>	
38	0.05	Ca	20	18	3.469(04)	[69, 70]	Ar	18	20	3.402(06)	
39	0.03	Ca	20	19	3.464(04)	[69, 70]	K	19	20	3.435(04)	
40	0.05	Sc	21	19	<i>3.508(04)</i>		K	19	21	3.439(04)	[68, 71, 72]
40	0.10	Ti	22	18	<i>3.566(06)</i>		Ar	18	22	3.427(04)	
41	0.02	Sc	21	20	<i>3.515(04)</i>		Ca	20	21	3.481(04)	[70, 73]
41	0.07	Ti	22	19	<i>3.556(06)</i>		K	19	22	3.455(05)	[68, 71, 72, 74]
42	0.05	Ti	22	20	<i>3.576(05)</i>		Ca	20	22	3.510(04)	[75]
42	0.14	Cr	24	18	<i>3.638(12)</i>		Ar	18	24	3.440(11)	[66] D
43	0.02	Ti	22	21	<i>3.583(12)</i>		Sc	21	22	3.550(11)	[76, 77] E
43	0.07	V	23	20	<i>3.594(05)</i>		Ca	20	23	3.497(04)	[75]
43	0.12	Cr	24	19	<i>3.620(09)</i>		K	19	24	3.459(08)	[68, 74]
44	0.05	V	23	21	<i>3.604(08)</i>		Sc	21	23	3.540(08)	[76, 77] E
44	0.09	Cr	24	20	<i>3.645(06)</i>		Ca	20	24	3.519(04)	[75]
45	0.02	V	23	22	<i>3.628(05)</i>		Ti	22	23	3.597(05)	[78]
45	0.07	Cr	24	21	<i>3.640(07)</i>		Sc	21	24	3.548(07)	
46	0.04	Cr	24	22	<i>3.670(05)</i>		Ti	22	24	3.610(04)	[78]
46	0.09	Mn	25	21	<i>3.651(09)</i>		Sc	21	25	3.530(08)	[76, 77] E
46	0.13	Fe	26	20	<i>3.677(07)</i>		Ca	20	26	3.497(04)	[75]
47	0.06	Mn	25	22	<i>3.688(05)</i>		Ti	22	25	3.599(04)	[78]
48	0.08	Fe	26	22	<i>3.710(05)</i>		Ti	22	26	3.595(04)	
49	0.02	Mn	25	24	<i>3.685(06)</i>		Cr	24	25	3.656(06)	[79]
50	0.04	Fe	26	24	<i>3.709(04)</i>		Cr	24	26	3.664(04)	
50	0.12	Ni	28	22	<i>3.738(06)</i>		Ti	22	28	3.572(04)	
51	0.02	Fe	26	25	<i>3.746(35)</i>		Mn	25	26	3.719(35)	[80, 81] F
51	0.06	Co	27	24	<i>3.718(05)</i>		Cr	24	27	3.637(04)	[79]
51	0.10	Ni	28	23	<i>3.734(06)</i>		V	23	28	3.598(04)	
52	0.04	Co	27	25	<i>3.728(27)</i>		Mn	25	27	3.675(27)	[80, 81] F
52	0.08	Ni	28	24	<i>3.750(05)</i>		Cr	24	28	3.644(04)	
53	0.02	Co	27	26	<i>3.727(07)</i>		Fe	26	27	3.701(07)	[82]
53	0.06	Ni	28	25	<i>3.745(22)</i>		Mn	25	28	3.667(22)	[80, 81] F
54	0.04	Ni	28	26	3.741(05)	[83]	Fe	26	28	3.688(04)	
55	0.02	Ni	28	27	3.691(05)	[84]	Co	27	28	<i>3.666(05)</i>	
56	0.07	Zn	30	26	<i>3.832(05)</i>		Fe	26	30	3.733(04)	
58	0.03	Zn	30	28	<i>3.820(03)</i>		Ni	28	30	3.773(03)	
59	0.02	Zn	30	29	<i>3.844(10)</i>		Cu	29	30	3.820(10)	[85]
60	0.03	Ga	31	29	<i>3.883(09)</i>		Cu	29	31	3.836(09)	[85]
60	0.07	Ge	32	28	<i>3.903(05)</i>		Ni	28	32	3.809(03)	[84]
61	0.05	Ge	32	29	<i>3.924(07)</i>		Cu	29	32	3.856(07)	[85]

**Table 5**

Charge radii of mirror nuclei. Known radii are taken from Tab. 2 along with isotopic differences taken from the indicated references. Predicted radii relying on the validity of Eq. 6 are given in italics.

A	I	el.	Z	N	r	Ref./Note	el.	Z	N	r	Ref./Note
62	0.03	Ge	32	30	<i>3.927(06)</i>		Zn	30	32	3.883(06)	[40, 86]
63	0.02	Ge	32	31	<i>3.955(19)</i>		Ga	31	32	3.933(19)	[87]
64	0.03	As	33	31	<i>3.984(17)</i>		Ga	31	33	3.941(17)	[87]
65	0.05	Se	34	31	<i>4.025(14)</i>		Ga	31	34	3.961(14)	[88]
74	0.03	Sr	38	36	<i>4.205(12)</i>		Kr	36	38	4.168(12)	[89, 90] G

A. The absolute radius of  $^{14}\text{C}$  was measured via muonic x-ray spectroscopy to be 2.496(19) fm [60]. It was quoted later with half of that uncertainty [6] which persisted through later compilations [7, 8]. The radius given in this work is obtained by combining that of  $^{12}\text{C}$  from [48] together with the radii difference from [60], for which the calibration uncertainty is reduced.

B. The difference  $r_{16} - r_{17} = 8(7)$  am was measured with electron scattering over a wide momentum transfer range analyzed (nearly) model-independently [61]. The following note indicates the reliability of this value.

C. The difference measured via muonic x-rays  $r_{18} - r_{16} = 76(5)$  am [62] agrees well with that measured with electron scattering  $r_{18} - r_{16} = 74(5)$  am [61].

D. The uncertainty in these radii is dominated by a 10% uncertainty assumed for a semi-empirically evaluated field shift factor. Experience shows that this uncertainty might be underestimated. See e.g. [25, 27–29, 42].

E. The optical isotope shift measurements of [76] were reanalyzed in [77] using more reliable IS factor calculations.

F. Systematic uncertainties related to the atomic factors, missing in a recent compilation [91], were extracted from Fig. 9 in [81] and added in quadrature.

G. The optical measurements of [89] were originally analyzed using a semi-empirical field shift factor assuming it has an uncertainty of 10%, which we believe to be underestimated (See note D). The extracted radius is given in [8] without the dominating systematic uncertainty. We opted for the analysis of [90] in which the atomic factors are extracted from a King plot.

**Table 6**

Re-calibration of the Sodium chain, whose optical isotope shifts are given in [33, 92–94], using  $F = -39.3(3)$  MHz/fm<sup>2</sup> [34] and  $K = 384.7(6)$  MHz/fm<sup>2</sup> whose estimation is described in the main text.

A	$\delta r^2$ fm <sup>2</sup>	$\sigma_{\text{exp}}$ fm <sup>2</sup>	$\sigma_{K,F}$ fm <sup>2</sup>	$\sigma_{\text{tot}}$ fm <sup>2</sup>	r fm	$\sigma_{\delta r}$ fm	$\sigma_{r23}$ fm	$\sigma_{\text{tot}}$ fm	Ref. [34] fm
20	-0.05	0.09	0.10	0.14	2.983	0.023	0.005	0.024	2.89(9)
21	0.22			0.05	3.029			0.006	2.97(6)
22	0.01	0.02	0.03	0.04	2.994	0.006	0.005	0.008	2.967(27)
23					2.992			0.005	2.994(4)
24	-0.17	0.04	0.03	0.05	2.963	0.009	0.005	0.010	2.990(26)
25	-0.18	0.05	0.05	0.07	2.963	0.012	0.005	0.013	3.013(48)
26	-0.09	0.02	0.08	0.08	2.977	0.014	0.005	0.015	3.049(68)
27	0.05	0.05	0.10	0.11	3.000	0.019	0.005	0.020	3.091(86)
28	0.23	0.07	0.12	0.14	3.030	0.023	0.005	0.024	3.14(10)
29	0.62	0.10	0.14	0.17	3.094	0.028	0.005	0.028	3.22(11)
30	0.81	0.15	0.16	0.22	3.125	0.035	0.005	0.036	3.26(13)
31	1.23	0.09	0.18	0.20	3.192	0.031	0.005	0.031	3.34(14)

**Table 7**

Radii of isotriplet nuclei.  $r_{\pm 1}$  are from Tab. 5,  $r_{0,SE}$ ,  $\Delta M_B^{(1)}$ , and  $r_{CW}$  are calculated using Eq. 9, Eq. 10, and 11, respectively. Asterisks denote short-lived excited nuclear states. “m” denotes long-lived nuclear isomers.  $r_{0,exp}$  are determined by combining reference radii from Tab. 2, optical isotopes shifts given in Refs. [76, 81, 95–97], and improved calculations of atomic factors from Refs. [41, 68, 77].

	$r_{-1}$ fm	$r_{0,SE}$ fm	$r_{0,exp}$ fm	$r_{+1}$ fm	$\Delta M_B^{(1)}$ fm <sup>2</sup>	$r_{CW}^2$ fm <sup>2</sup>	Ref. [38]
${}^{10}_6\text{C}$	2.638(36)	${}^{10}_5\text{B}^*$ 2.531(38)		${}^{10}_4\text{Be}$ 2.361(36)		9.72(25)	N/A
${}^{14}_8\text{O}$	2.706(11)	${}^{14}_7\text{N}^*$ 2.623(10)		${}^{14}_6\text{C}$ 2.508(09)		10.41(12)	N/A
${}^{18}_{10}\text{Ne}$	2.934(09)	${}^{18}_9\text{F}^*$ 2.863(07)		${}^{18}_8\text{O}$ 2.777(07)		12.08(12)	13.4(5)
${}^{22}_{12}\text{Mg}$	3.071(05)	${}^{22}_{11}\text{Na}^*$ 3.017(05)		${}^{22}_{10}\text{Ne}$ 2.948(04)		13.24(12)	12.9(7)
${}^{26}_{14}\text{Si}$	3.137(04)	${}^{26}_{13}m\text{Al}$ 3.088(04)	3.132(08)	${}^{26}_{12}\text{Mg}$ 3.030(03)	−3.5(0.7)	13.77(12)	N/A
${}^{30}_{16}\text{S}$	3.224(07)	${}^{30}_{15}\text{P}^*$ 3.181(06)		${}^{30}_{14}\text{Si}$ 3.132(06)		14.50(13)	N/A
${}^{34}_{18}\text{Ar}$	3.365(11)	${}^{34}_{17}\text{Cl}$ 3.328(04)		${}^{34}_{16}\text{S}$ 3.284(04)		15.66(13)	15.6(5)
${}^{38}_{20}\text{Ca}$	3.469(04)	${}^{38}_{19}m\text{K}$ 3.440(07)	3.437(05)	${}^{38}_{18}\text{Ar}$ 3.402(06)	0.6(1.1)	16.58(13)	16.0(3)
${}^{42}_{22}\text{Ti}$	3.576(05)	${}^{42}_{21}\text{Sc}$ 3.545(04)	3.558(16)	${}^{42}_{20}\text{Ca}$ 3.510(04)	−2.0(2.4)	17.46(13)	21.5(3.6)
${}^{46}_{24}\text{Cr}$	3.670(05)	${}^{46}_{23}\text{V}$ 3.642(05)		${}^{46}_{22}\text{Ti}$ 3.610(04)		18.29(14)	N/A
${}^{50}_{26}\text{Fe}$	3.719(04)	${}^{50}_{25}\text{Mn}$ 3.693(04)	3.728(41)	${}^{50}_{24}\text{Cr}$ 3.664(04)	−6.6(7.8)	18.73(14)	23.2(3.8)
${}^{54}_{28}\text{Ni}$	3.741(05)	${}^{54}_{27}\text{Co}$ 3.715(04)		${}^{54}_{26}\text{Fe}$ 3.688(04)		18.93(14)	18.3(9)
${}^{58}_{30}\text{Zn}$	3.820(03)	${}^{58}_{29}\text{Cu}^*$ 3.797(03)		${}^{58}_{28}\text{Ni}$ 3.773(03)		19.66(14)	N/A
${}^{62}_{32}\text{Ge}$	3.927(06)	${}^{62}_{31}\text{Ga}$ 3.906(06)		${}^{62}_{30}\text{Zn}$ 3.883(06)		20.65(15)	N/A
${}^{74}_{38}\text{Sr}$	4.205(12)	${}^{74}_{37}\text{Rb}$ 4.187(12)	4.194(17)	${}^{74}_{36}\text{Kr}$ 4.168(12)	−1.9(6.5)	23.32(19)	19.5(5.5)

## References

- [1] Gerhard Fricke, K Heilig, and Herwig F Schopper. Nuclear charge radii. 2004.
- [2] W Nörtershäuser and ID Moore. Nuclear charge radii. In *Handbook of Nuclear Physics*, pages 1–70. Springer, 2022.
- [3] R.C. Barrett. Model-independent parameters of the nuclear charge distribution from muonic x-rays. *Physics Letters B*, 33(6):388–390, 1970. ISSN 0370-2693. doi: [https://doi.org/10.1016/0370-2693\(70\)90611-8](https://doi.org/10.1016/0370-2693(70)90611-8). URL <https://www.sciencedirect.com/science/article/pii/0370269370906118>.
- [4] G. Fricke, C. Bernhardt, K. Heilig, L.A. Schaller, L. Schellenberg, E.B. Shera, and C.W. Dejager. Nuclear ground state charge radii from electromagnetic interactions. *Atomic Data and Nuclear Data Tables*, 60(2):177–285, 1995. ISSN 0092-640X. doi: <https://doi.org/10.1006/adnd.1995.1007>. URL <https://www.sciencedirect.com/science/article/pii/S0092640X85710078>.
- [5] Ben Ohayon, Andreas Abeln, Silvia Bara, Thomas Elias Cocolios, Ofir Eizenberg, Andreas Fleischmann, Loredana Gastaldo, César Godinho, Michael Heines, Daniel Hengstler, et al. Towards precision muonic x-ray measurements of charge radii of light nuclei. *Physics*, 6(1):206–215, 2024.
- [6] I Angeli. Table of nuclear root mean square charge radii, Sep 1999.
- [7] I. Angeli. A consistent set of nuclear rms charge radii: properties of the radius surface  $r(n,z)$ . *Atomic Data and Nuclear Data Tables*, 87(2):185–206, 2004. ISSN 0092-640X. doi: <https://doi.org/10.1016/j.adt.2004.04.002>. URL <https://www.sciencedirect.com/science/article/pii/S0092640X04000166>.
- [8] I. Angeli and K.P. Marinova. Table of experimental nuclear ground state charge radii: An update. *Atomic Data and Nuclear Data Tables*, 99(1):69–95, 2013. ISSN 0092-640X. doi: <https://doi.org/10.1016/j.adt.2011.12.006>. URL <https://www.sciencedirect.com/science/article/pii/S0092640X12000265>.
- [9] H. Heylen, C. S. Devlin, W. Gins, M. L. Bissell, K. Blaum, B. Cheal, L. Filippin, R. F. Garcia Ruiz, M. Godefroid, C. Gorges, J. D. Holt, A. Kanellakopoulos, S. Kaufmann, Á. Koszorús, K. König, S. Malbrunot-Ettenauer, T. Miyagi, R. Neugart, G. Neyens, W. Nörtershäuser, R. Sánchez, F. Sommer, L. V. Rodríguez, L. Xie, Z. Y. Xu, X. F. Yang, and D. T. Yordanov. High-resolution laser spectroscopy of  $^{27-32}\text{Al}$ . *Phys. Rev. C*, 103:014318, Jan 2021. doi: 10.1103/PhysRevC.103.014318. URL <https://link.aps.org/doi/10.1103/PhysRevC.103.014318>.
- [10] R.M. Lombard and G.R. Bishop. The scattering of high-energy electrons by  $^{27}\text{Al}$ . *Nuclear Physics A*, 101(3):601–624, 1967. ISSN 0375-9474. doi: [https://doi.org/10.1016/0375-9474\(67\)90655-0](https://doi.org/10.1016/0375-9474(67)90655-0). URL <https://www.sciencedirect.com/science/article/pii/0375947467906550>.
- [11] G Fey, H Frank, W Schütz, and H Theissen. Nuclear rms charge radii from relative electron scattering measurements at low energies. *Zeitschrift für Physik*, 265:401–403, 1973.
- [12] H. De Vries, C.W. De Jager, and C. De Vries. Nuclear Charge-Density-Distribution Parameters from Elastic Electron Scattering. 36(3):495, 1987. URL <http://www.sciencedirect.com/science/article/pii/0092640X87900131>.
- [13] Ingo Sick. Form Factors and Radii of Light Nuclei. *Journal of Physical and Chemical Reference Data*, 44(3):031213, 06 2015. ISSN 0047-2689. doi: 10.1063/1.4921830. URL <https://doi.org/10.1063/1.4921830>.
- [14] J. Wesseling, C. W. de Jager, L. Lapikás, H. de Vries, L. W. Fagg, M. N. Harakeh, N. Kalantar-Nayestanaki, R. A. Lindgren, E. Moya De Guerra, and P. Sarriguren.  $2s_{1/2}$  occupancies in  $^{30}\text{Si}$ ,  $^{31}\text{P}$ , and  $^{32}\text{S}$ . *Phys. Rev. C*, 55:2773–2786, Jun 1997. doi: 10.1103/PhysRevC.55.2773. URL <https://link.aps.org/doi/10.1103/PhysRevC.55.2773>.
- [15] Atakan Çavuşoğlu and Bastian Sikora. Impact of the nuclear charge distribution on the g-factors and ground state energies of bound muons. *arXiv preprint arXiv:2311.16855*, 2023.
- [16] W. Ruckstuhl, B. Aas, W. Beer, I. Beltrami, F. W. N. de Boer, K. Bos, P. F. A. Goudsmit, U. Kiebele, H. J. Leisi, G. Strassner, A. Vacchi, and R. Weber. High-Precision Muonic X-Ray Measurement of the rms Charge Radius of  $^{12}\text{C}$  with a Crystal Spectrometer. *Physical Review Letters*, 49(12):859–862, 1982. doi: 10.1103/PhysRevLett.49.859. URL <https://link.aps.org/doi/10.1103/PhysRevLett.49.859>. PRL.
- [17] G. Fricke and K. Heilig. Nuclear charge radii · 6-c carbon: Datasheet from landolt-börnstein - group i elementary particles, nuclei and atoms · volume 20: “nuclear charge radii” in springer materials (<https://doi.org/10.1007/10856314-8>), . URL [https://materials.springer.com/lb/docs/sm\\_lbs\\_978-3-540-45555-4\\_8](https://materials.springer.com/lb/docs/sm_lbs_978-3-540-45555-4_8). Copyright 2004 Springer-Verlag Berlin Heidelberg.
- [18] X.F. Yang, S.J. Wang, S.G. Wilkins, and R.F. Garcia Ruiz. Laser spectroscopy for the study of exotic nuclei. *Progress in Particle and Nuclear Physics*, 129:104005, 2023. ISSN 0146-6410. doi: <https://doi.org/10.1016/j.pnpnp.2022.104005>. URL <https://www.sciencedirect.com/science/article/pii/S0146641022000631>.

- [19] B. K. Sahoo, S. Blundell, A. V. Oleynichenko, R. F. Garcia Ruiz, L. V. Skripnikov, and B. Ohayon. Recent advancements in atomic many-body methods for high-precision studies of isotope shifts. 2024. URL <https://arxiv.org/abs/2408.09959>.
- [20] W. Geithner, T. Neff, G. Audi, K. Blaum, P. Delahaye, H. Feldmeier, S. George, C. Guénaut, F. Herfurth, A. Herlert, S. Kappertz, M. Keim, A. Kellerbauer, H.-J. Kluge, M. Kowalska, P. Lievens, D. Lunney, K. Marinova, R. Neugart, L. Schweikhard, S. Wilbert, and C. Yazidjian. Masses and charge radii of  $^{17-22}\text{Ne}$  and the two-proton-halo candidate  $^{17}\text{Ne}$ . *Phys. Rev. Lett.*, 101:252502, Dec 2008. doi: 10.1103/PhysRevLett.101.252502. URL <https://link.aps.org/doi/10.1103/PhysRevLett.101.252502>.
- [21] K. Marinova, W. Geithner, M. Kowalska, K. Blaum, S. Kappertz, M. Keim, S. Kloos, G. Kotrotsios, P. Lievens, R. Neugart, H. Simon, and S. Wilbert. Charge radii of neon isotopes across the *sd* neutron shell. *Phys. Rev. C*, 84:034313, Sep 2011. doi: 10.1103/PhysRevC.84.034313. URL <https://link.aps.org/doi/10.1103/PhysRevC.84.034313>.
- [22] G. Fricke and K. Heilig. Nuclear charge radii · 10-ne neon: Datasheet from landolt-börnstein - group i elementary particles, nuclei and atoms · volume 20: “nuclear charge radii” in springer materials ([https://doi.org/10.1007/10856314\\_12](https://doi.org/10.1007/10856314_12)), . URL [https://materials.springer.com/lb/docs/sm\\_lbs\\_978-3-540-45555-4\\_12](https://materials.springer.com/lb/docs/sm_lbs_978-3-540-45555-4_12). Copyright 2004 Springer-Verlag Berlin Heidelberg.
- [23] E A Knight, R P Singhal, R G Arthur, and M W S Macauley. Elastic scattering of electrons from  $^{20,22}\text{Ne}$ . *Journal of Physics G: Nuclear Physics*, 7(8):1115, aug 1981. doi: 10.1088/0305-4616/7/8/017. URL <https://dx.doi.org/10.1088/0305-4616/7/8/017>.
- [24] J. R. Moreira, R. P. Singhal, and H. S. Caplan. Charge radii of  $^{20, 22}\text{Ne}$  determined from elastic electron scattering. *Canadian Journal of Physics*, 49(11):1434–1436, 1971. doi: 10.1139/p71-169. URL <https://doi.org/10.1139/p71-169>.
- [25] B. Ohayon, H. Rahangdale, A. J. Geddes, J. C. Berengut, and G. Ron. Isotope shifts in  $^{20,22}\text{Ne}$ : Precision measurements and global analysis in the framework of intermediate coupling. *Phys. Rev. A*, 99:042503, Apr 2019. doi: 10.1103/PhysRevA.99.042503. URL <https://link.aps.org/doi/10.1103/PhysRevA.99.042503>.
- [26] Amy Geddes. *Searching for New Interactions Between Nuclei and Electrons at the Precision Frontier*. PhD thesis, UNSW Sydney, 2021.
- [27] G. Torbohm, B. Fricke, and A. Rosén. State-dependent volume isotope shifts of low-lying states of group-ii and -iib elements. *Phys. Rev. A*, 31:2038–2053, Apr 1985. doi: 10.1103/PhysRevA.31.2038. URL <https://link.aps.org/doi/10.1103/PhysRevA.31.2038>.
- [28] Ann-Marie Mårtensson-Pendrill, Anders Ynnerman, Håkan Warston, Ludo Vermeeren, Roger E. Silverans, Alexander Klein, Rainer Neugart, Christoph Schulz, Peter Lievens, and The ISOLDE Collaboration. Isotope shifts and nuclear-charge radii in singly ionized  $^{40-48}\text{Ca}$ . *Phys. Rev. A*, 45:4675–4681, Apr 1992. doi: 10.1103/PhysRevA.45.4675. URL <https://link.aps.org/doi/10.1103/PhysRevA.45.4675>.
- [29] Magdalena Kowalska. *Ground state properties of neutron-rich Mg isotopes: the “island of inversion” studied with laser and  $\beta$ -NMR spectroscopy*. PhD thesis, Mainz U., Inst. Phys., 2006.
- [30] Tim Sailer, Vincent Debierre, Zoltán Harman, Fabian Heiße, Charlotte König, Jonathan Morgner, Bingsheng Tu, Andrey V Volotka, Christoph H Keitel, Klaus Blaum, et al. Measurement of the bound-electron g-factor difference in coupled ions. *Nature*, 606(7914):479–483, 2022.
- [31] S. J. Novario, D. Lonardonì, S. Gandolfi, and G. Hagen. Trends of neutron skins and radii of mirror nuclei from first principles. *Phys. Rev. Lett.*, 130:032501, Jan 2023. doi: 10.1103/PhysRevLett.130.032501. URL <https://link.aps.org/doi/10.1103/PhysRevLett.130.032501>.
- [32] B. Cheal, T. E. Cocolios, and S. Fritzsche. Laser spectroscopy of radioactive isotopes: Role and limitations of accurate isotope-shift calculations. *Phys. Rev. A*, 86:042501, Oct 2012. doi: 10.1103/PhysRevA.86.042501. URL <https://link.aps.org/doi/10.1103/PhysRevA.86.042501>.
- [33] G. Huber, F. Touchard, S. Büttgenbach, C. Thibault, R. Klapisch, H. T. Duong, S. Liberman, J. Pinard, J. L. Vialle, P. Juncar, and P. Jacquinet. Spins, magnetic moments, and isotope shifts of  $^{21-31}\text{Na}$  by high resolution laser spectroscopy of the atomic  $D_1$  line. *Phys. Rev. C*, 18:2342–2354, Nov 1978. doi: 10.1103/PhysRevC.18.2342. URL <https://link.aps.org/doi/10.1103/PhysRevC.18.2342>.
- [34] B. Ohayon, R. F. Garcia Ruiz, Z. H. Sun, G. Hagen, T. Papenbrock, and B. K. Sahoo. Nuclear charge radii of na isotopes: Interplay of atomic and nuclear theory. *Phys. Rev. C*, 105:L031305, Mar 2022. doi: 10.1103/PhysRevC.105.L031305. URL <https://link.aps.org/doi/10.1103/PhysRevC.105.L031305>.

- [35] J. C. Hardy and I. S. Towner. Superaligned  $0^+ \rightarrow 0^+$  nuclear  $\beta$  decays: 2020 critical survey, with implications for  $V_{ud}$  and ckm unitarity. *Phys. Rev. C*, 102:045501, Oct 2020. doi: 10.1103/PhysRevC.102.045501. URL <https://link.aps.org/doi/10.1103/PhysRevC.102.045501>.
- [36] Chien-Yeah Seng and Mikhail Gorchtein. Data-driven re-evaluation of  $ft$ -values in superallowed beta decays. *arXiv preprint arXiv:2309.16893*, 2023.
- [37] Chien-Yeah Seng and Mikhail Gorchtein. Electroweak nuclear radii constrain the isospin breaking correction to  $v_{ud}$ . *Physics Letters B*, 838:137654, 2023. ISSN 0370-2693. doi: <https://doi.org/10.1016/j.physletb.2022.137654>. URL <https://www.sciencedirect.com/science/article/pii/S0370269322007882>.
- [38] Chien-Yeah Seng. Model-independent determination of nuclear weak form factors and implications for standard model precision tests. *Phys. Rev. Lett.*, 130:152501, Apr 2023. doi: 10.1103/PhysRevLett.130.152501. URL <https://link.aps.org/doi/10.1103/PhysRevLett.130.152501>.
- [39] Livio Filippin, Randolph Beerwerth, Jörgen Ekman, Stephan Fritzsche, Michel Godefroid, and Per Jönsson. Multiconfiguration calculations of electronic isotope shift factors in al i. *Phys. Rev. A*, 94:062508, Dec 2016. doi: 10.1103/PhysRevA.94.062508. URL <https://link.aps.org/doi/10.1103/PhysRevA.94.062508>.
- [40] BK Sahoo and B Ohayon. All-optical differential radii in zinc. *arXiv preprint arXiv:2307.09092*, 2023.
- [41] Leonid V. Skripnikov, Sergey D. Prosnjak, Aleksei V. Malyshev, Michail Athanasakis-Kaklamanakis, Alex Jose Brinson, Kei Minamisono, Fabian C. Pastrana Cruz, Jordan Ray Reilly, Brooke J. Rickey, and Ronald F. Garcia Ruiz. Isotope-shift factors with quantum electrodynamics effects for many-electron systems: A study of the nuclear charge radius of  $^{26m}\text{Al}$ . *Phys. Rev. A*, 110:012807, Jul 2024. doi: 10.1103/PhysRevA.110.012807. URL <https://link.aps.org/doi/10.1103/PhysRevA.110.012807>.
- [42] B Ohayon, JE Padilla-Castillo, SC Wright, G Meijer, and BK Sahoo. Reconciling differential radii in the silver chain through improved measurement and  $\{ \backslash \text{it ab initio} \}$  calculations. *arXiv preprint arXiv:2402.07618*, 2024.
- [43] Michael Heines, Luke Antwis, Silvia Bara, Bart Caerts, Thomas E. Cocolios, Stefan Eisenwinder, Julian Fletcher, Tom Kieck, Andreas Knecht, Megumi Niikura, Narongrit Ritjoho, Lino M.C. Pereira, Randolph Pohl, André Vantomme, Stergiani M. Vogiatzi, Katharina von Schoeler, Frederik Wauters, Roger Webb, Qiang Zhao, and Sami Zweidler. Muonic x-ray spectroscopy on implanted targets. *Nuclear Instruments and Methods in Physics Research Section B: Beam Interactions with Materials and Atoms*, 541:173–175, 2023. ISSN 0168-583X. doi: <https://doi.org/10.1016/j.nimb.2023.05.036>. URL <https://www.sciencedirect.com/science/article/pii/S0168583X23002410>.
- [44] D. Rychel, H.J. Emrich, H. Miska, R. Gyufko, and C.A. Wiedner. Charge distribution of the seven sulphur isotopes from elastic electron scattering. *Physics Letters B*, 130(1):5–8, 1983. ISSN 0370-2693. doi: [https://doi.org/10.1016/0370-2693\(83\)91051-1](https://doi.org/10.1016/0370-2693(83)91051-1). URL <https://www.sciencedirect.com/science/article/pii/0370269383910511>.
- [45] W. Nörtershäuser, T. Neff, R. Sánchez, and I. Sick. Charge radii and ground state structure of lithium isotopes: Experiment and theory reexamined. *Phys. Rev. C*, 84:024307, Aug 2011. doi: 10.1103/PhysRevC.84.024307. URL <https://link.aps.org/doi/10.1103/PhysRevC.84.024307>.
- [46] J.A. Jansen, R.Th. Peerdeman, and C. De Vries. Nuclear charge radii of  $^{12}\text{C}$  and  $^9\text{Be}$ . *Nuclear Physics A*, 188(2):337–352, 1972. ISSN 0375-9474. doi: [https://doi.org/10.1016/0375-9474\(72\)90062-0](https://doi.org/10.1016/0375-9474(72)90062-0). URL <https://www.sciencedirect.com/science/article/pii/0375947472900620>.
- [47] B.M. Barnett, W. Gyles, R.R. Johnson, K.L. Erdman, J. Johnstone, J.J. Kraushaar, S. Lepp, T.G. Masterson, E. Rost, D.R. Gill, A.W. Thomas, J. Alster, I. Navon, and R.H. Landau. Proton radii determinations from the ratio of  $\pi^+$  elastic scattering from  $^{11}\text{B}$  and  $^{12}\text{C}$ . *Physics Letters B*, 97(1):45–49, 1980. ISSN 0370-2693. doi: [https://doi.org/10.1016/0370-2693\(80\)90543-2](https://doi.org/10.1016/0370-2693(80)90543-2). URL <https://www.sciencedirect.com/science/article/pii/0370269380905432>.
- [48] W. Ruckstuhl, B. Aas, W. Beer, I. Beltrami, K. Bos, P.F.A. Goudsmit, H.J. Leisi, G. Strassner, A. Vacchi, F.W.N. De Boer, U. Kiebele, and R. Weber. Precision measurement of the 2p-1s transition in muonic  $^{12}\text{C}$ : Search for new muon-nucleon interactions or accurate determination of the rms nuclear charge radius. *Nuclear Physics A*, 430(3):685–712, 1984. ISSN 0375-9474. doi: [https://doi.org/10.1016/0375-9474\(84\)90101-5](https://doi.org/10.1016/0375-9474(84)90101-5). URL <https://www.sciencedirect.com/science/article/pii/0375947484901015>.
- [49] E. A. J. M. Offermann, L. S. Cardman, C. W. de Jager, H. Miska, C. de Vries, and H. de Vries. Energy dependence of the form factor for elastic electron scattering from  $^{12}\text{C}$ . *Phys. Rev. C*, 44:1096–1117, Sep 1991. doi: 10.1103/PhysRevC.44.1096. URL <https://link.aps.org/doi/10.1103/PhysRevC.44.1096>.
- [50] J.W. de Vries, D. Doornhof, C.W. de Jager, R.P. Singhal, S. Salem, G.A. Peterson, and R.S. Hicks. The  $^{15}\text{N}$  ground state studied with elastic electron scattering. *Physics Letters B*, 205(1):22–25, 1988. ISSN 0370-2693. doi:

[https://doi.org/10.1016/0370-2693\(88\)90392-9](https://doi.org/10.1016/0370-2693(88)90392-9). URL <https://www.sciencedirect.com/science/article/pii/S0370269388903929>.

- [51] G. Fricke and K. Heilig. Nuclear charge radii · 8-o oxygen: Datasheet from landolt-börnstein - group i elementary particles, nuclei and atoms · volume 20: “nuclear charge radii” in springer materials ([https://doi.org/10.1007/10856314\\_10](https://doi.org/10.1007/10856314_10)), . URL [https://materials.springer.com/lb/docs/sm\\_lbs\\_978-3-540-45555-4\\_10](https://materials.springer.com/lb/docs/sm_lbs_978-3-540-45555-4_10). Copyright 2004 Springer-Verlag Berlin Heidelberg.
- [52] G. Backenstoss, S. Charalambus, H. Daniel, H. Koch, G. Poelz, H. Schmitt, and L. Tauscher. Nuclear radii of light nuclei from muonic x-ray measurements. *Physics Letters B*, 25(9):547–549, 1967. ISSN 0370-2693. doi: [https://doi.org/10.1016/0370-2693\(67\)90142-6](https://doi.org/10.1016/0370-2693(67)90142-6). URL <https://www.sciencedirect.com/science/article/pii/S0370269367901426>.
- [53] W.J. Briscoe, Hall Crannell, and J.C. Bergstrom. Elastic electron scattering from the isotopes  $^{35}\text{Cl}$  and  $^{37}\text{Cl}$ . *Nuclear Physics A*, 344(3):475–488, 1980. ISSN 0375-9474. doi: [https://doi.org/10.1016/0375-9474\(80\)90402-9](https://doi.org/10.1016/0375-9474(80)90402-9). URL <https://www.sciencedirect.com/science/article/pii/S0375947480904029>.
- [54] H. D. Wohlfahrt, O. Schwentker, G. Fricke, H. G. Andresen, and E. B. Shera. Systematics of nuclear charge distributions in the mass 60 region from elastic electron scattering and muonic x-ray measurements. *Phys. Rev. C*, 22: 264–283, Jul 1980. doi: 10.1103/PhysRevC.22.264. URL <https://link.aps.org/doi/10.1103/PhysRevC.22.264>.
- [55] W. Nörtershäuser, D. Tiedemann, M. Žáková, Z. Andjelkovic, K. Blaum, M. L. Bissell, R. Cazan, G. W. F. Drake, Ch. Geppert, M. Kowalska, J. Krämer, A. Krieger, R. Neugart, R. Sánchez, F. Schmidt-Kaler, Z.-C. Yan, D. T. Yordanov, and C. Zimmermann. Nuclear Charge Radii of  $^{7,9,10}\text{Be}$  and the One-Neutron Halo Nucleus  $^{11}\text{Be}$ . *Phys. Rev. Lett.*, 102:062503, Feb 2009. doi: 10.1103/PhysRevLett.102.062503. URL <https://link.aps.org/doi/10.1103/PhysRevLett.102.062503>.
- [56] Craig J. Sansonetti, C. E. Simien, J. D. Gillaspay, Joseph N. Tan, Samuel M. Brewer, Roger C. Brown, Saijun Wu, and J. V. Porto. Absolute transition frequencies and quantum interference in a frequency comb based measurement of the  $^{6,7}\text{Li}$   $d$  lines. *Phys. Rev. Lett.*, 107:023001, Jul 2011. doi: 10.1103/PhysRevLett.107.023001. URL <https://link.aps.org/doi/10.1103/PhysRevLett.107.023001>.
- [57] Roger C. Brown, Saijun Wu, J. V. Porto, Craig J. Sansonetti, C. E. Simien, Samuel M. Brewer, Joseph N. Tan, and J. D. Gillaspay. Quantum interference and light polarization effects in unresolvable atomic lines: Application to a precise measurement of the  $^{6,7}\text{Li}$   $D_2$  lines. *Phys. Rev. A*, 87:032504, Mar 2013. doi: 10.1103/PhysRevA.87.032504. URL <https://link.aps.org/doi/10.1103/PhysRevA.87.032504>.
- [58] W. Nörtershäuser, R. Sánchez, G. Ewald, A. Dax, J. Behr, P. Bricault, B. A. Bushaw, J. Dilling, M. Döbbsky, G. W. F. Drake, S. Götze, H.-J. Kluge, Th. Kühl, J. Lassen, C. D. P. Levy, K. Pachucki, M. Pearson, M. Puchalski, A. Wojtaszek, Z.-C. Yan, and C. Zimmermann. Isotope-shift measurements of stable and short-lived lithium isotopes for nuclear-charge-radii determination. *Phys. Rev. A*, 83:012516, Jan 2011. doi: 10.1103/PhysRevA.83.012516. URL <https://link.aps.org/doi/10.1103/PhysRevA.83.012516>.
- [59] Patrick Matthias Müller. *Laserspectroscopic determination of the nuclear charge radius of  $^{12}\text{C}$* . PhD thesis, Technische Universität Darmstadt, Darmstadt, March 2024. URL <http://tuprints.ulb.tu-darmstadt.de/26746/>.
- [60] L.A. Schaller, L. Schellenberg, T.Q. Phan, G. Piller, A. Ruetschi, and H. Schneuwly. Nuclear charge radii of the carbon isotopes  $^{12}\text{C}$ ,  $^{13}\text{C}$  and  $^{14}\text{C}$ . *Nuclear Physics A*, 379(3):523–535, 1982. ISSN 0375-9474. doi: [https://doi.org/10.1016/0375-9474\(82\)90012-4](https://doi.org/10.1016/0375-9474(82)90012-4). URL <https://www.sciencedirect.com/science/article/pii/S0375947482900124>.
- [61] H. Miska, B. Norum, M.V. Hynes, W. Bertozzi, S. Kowalski, F.N. Rad, C.P. Sargent, T. Sasanuma, and B.L. Berman. Precise measurement of the charge-distribution differences of the oxygen isotopes. *Physics Letters B*, 83(2):165–168, 1979. ISSN 0370-2693. doi: [https://doi.org/10.1016/0370-2693\(79\)90676-2](https://doi.org/10.1016/0370-2693(79)90676-2). URL <https://www.sciencedirect.com/science/article/pii/S0370269379906762>.
- [62] G. Backenstoss, W. Kowald, I. Schwanner, L. Tauscher, H.J. Weyer, D. Gotta, and R. Guigas. Precision determination of the difference of the charge radii of  $^{16}\text{O}$  and  $^{18}\text{O}$ . *Physics Letters B*, 95(2):212–214, 1980. ISSN 0370-2693. doi: [https://doi.org/10.1016/0370-2693\(80\)90471-2](https://doi.org/10.1016/0370-2693(80)90471-2). URL <https://www.sciencedirect.com/science/article/pii/S0370269380904712>.
- [63] D. T. Yordanov, M. L. Bissell, K. Blaum, M. De Rydt, Ch. Geppert, M. Kowalska, J. Krämer, K. Kreim, A. Krieger, P. Lievens, T. Neff, R. Neugart, G. Neyens, W. Nörtershäuser, R. Sánchez, and P. Vingerhoets. Nuclear charge radii of  $^{21-32}\text{Mg}$ . *Phys. Rev. Lett.*, 108:042504, Jan 2012. doi: 10.1103/PhysRevLett.108.042504. URL <https://link.aps.org/doi/10.1103/PhysRevLett.108.042504>.
- [64] Kristian König, Julian C Berengut, Anastasia Borschevsky, Alex Brinson, B Alex Brown, Adam Dockery, Serdar

- Elhatisari, Ephraim Eliav, Ronald F Garcia Ruiz, Jason D Holt, et al. Nuclear charge radii of silicon isotopes. *arXiv preprint arXiv:2309.02037*, 2023.
- [65] A. Klein, B.A. Brown, U. Georg, M. Keim, P. Lievens, R. Neugart, M. Neuroth, R.E. Silverans, L. Vermeeren, and ISOLDE Collaboration. Moments and mean square charge radii of short-lived argon isotopes. *Nuclear Physics A*, 607(1):1–22, 1996. ISSN 0375-9474. doi: [https://doi.org/10.1016/0375-9474\(96\)00192-3](https://doi.org/10.1016/0375-9474(96)00192-3). URL <https://www.sciencedirect.com/science/article/pii/0375947496001923>.
- [66] K. Blaum, W. Geithner, J. Lassen, P. Lievens, K. Marinova, and R. Neugart. Nuclear moments and charge radii of argon isotopes between the neutron-shell closures  $n=20$  and  $n=28$ . *Nuclear Physics A*, 799(1):30–45, 2008. ISSN 0375-9474. doi: <https://doi.org/10.1016/j.nuclphysa.2007.11.004>. URL <https://www.sciencedirect.com/science/article/pii/S0375947407007841>.
- [67] D. M. Rossi, K. Minamisono, H. B. Asberry, G. Bollen, B. A. Brown, K. Cooper, B. Isherwood, P. F. Mantica, A. Miller, D. J. Morrissey, R. Ringle, J. A. Rodriguez, C. A. Ryder, A. Smith, R. Strum, and C. Sumithrarachchi. Charge radii of neutron-deficient  $^{36}\text{K}$  and  $^{37}\text{K}$ . *Phys. Rev. C*, 92:014305, Jul 2015. doi: 10.1103/PhysRevC.92.014305. URL <https://link.aps.org/doi/10.1103/PhysRevC.92.014305>.
- [68] Á Koszorús, XF Yang, WG Jiang, SJ Novario, SW Bai, J Billowes, CL Binnersley, ML Bissell, Thomas Elias Cocolios, BS Cooper, et al. Charge radii of exotic potassium isotopes challenge nuclear theory and the magic character of  $N=32$ . *Nature Physics*, 17(4):439–443, 2021.
- [69] A Klose, C Kujawa, JD Lantis, B Maaß, PF Mantica, W Nazarewicz, et al. Proton superfluidity and charge radii in proton-rich calcium isotopes. *Nature physics*, 15(5):432–436, 2019.
- [70] A. Kramida. Isotope shifts in neutral and singly-ionized calcium. *Atomic Data and Nuclear Data Tables*, 133-134:101322, 2020. ISSN 0092-640X. doi: <https://doi.org/10.1016/j.adt.2019.101322>. URL <https://www.sciencedirect.com/science/article/pii/S0092640X19300853>.
- [71] H Schnatz, G Grosche, E Tiemann, Ch Lisdat, et al. The transition frequencies of the d lines of 39k, 40k, and 41k measured with a femtosecond laser frequency comb. In *Conference on Lasers and Electro-Optics*, page JTuD61. Optica Publishing Group, 2006.
- [72] Dipankar Das and Vasant Natarajan. High-precision measurement of hyperfine structure in the d lines of alkali atoms. *Journal of Physics B: Atomic, Molecular and Optical Physics*, 41(3):035001, jan 2008. doi: 10.1088/0953-4075/41/3/035001. URL <https://dx.doi.org/10.1088/0953-4075/41/3/035001>.
- [73] C W P Palmer, P E G Baird, S A Blundell, J R Brandenberger, C J Foot, D N Stacey, and G K Woodgate. Laser spectroscopy of calcium isotopes. *Journal of Physics B: Atomic and Molecular Physics*, 17(11):2197, jun 1984. doi: 10.1088/0022-3700/17/11/014. URL <https://dx.doi.org/10.1088/0022-3700/17/11/014>.
- [74] F. Touchard, P. Guimbal, S. Büttgenbach, R. Klapisch, M. De Saint Simon, J.M. Serre, C. Thibault, H.T. Duong, P. Juncar, S. Liberman, J. Pinard, and J.L. Vialle. Isotope shifts and hyperfine structure of 38–47k by laser spectroscopy. *Physics Letters B*, 108(3):169–171, 1982. ISSN 0370-2693. doi: [https://doi.org/10.1016/0370-2693\(82\)91167-4](https://doi.org/10.1016/0370-2693(82)91167-4). URL <https://www.sciencedirect.com/science/article/pii/0370269382911674>.
- [75] Patrick Müller, Kristian König, Phillip Imgram, Jörg Krämer, and Wilfried Nörtershäuser. Collinear laser spectroscopy of  $\text{Ca}^+$ : Solving the field-shift puzzle of the  $4s^2S_{1/2} \rightarrow 4p^2P_{1/2,3/2}$  transitions. *Phys. Rev. Res.*, 2:043351, Dec 2020. doi: 10.1103/PhysRevResearch.2.043351. URL <https://link.aps.org/doi/10.1103/PhysRevResearch.2.043351>.
- [76] M Avgoulea, Yu P Gangrsky, K P Marinova, S G Zemlyanoi, S Fritzsche, D Iablonskyi, C Barbieri, E C Simpson, P D Stevenson, J Billowes, P Campbell, B Cheal, B Tordoff, M L Bissell, D H Forest, M D Gardner, G Tungate, J Huikari, A Nieminen, H Penttilä, and J Äystö. Nuclear charge radii and electromagnetic moments of radioactive scandium isotopes and isomers. *Journal of Physics G: Nuclear and Particle Physics*, 38(2):025104, jan 2011. doi: 10.1088/0954-3899/38/2/025104. URL <https://dx.doi.org/10.1088/0954-3899/38/2/025104>.
- [77] Kristian König, Stephan Fritzsche, Gaute Hagen, Jason D. Holt, Andrew Klose, Jeremy Lantis, Yuan Liu, Kei Minamisono, Takayuki Miyagi, Witold Nazarewicz, Thomas Papenbrock, Skyy V. Pineda, Robert Powel, and Paul-Gerhard Reinhard. Surprising charge-radius kink in the sc isotopes at  $n=20$ . *Phys. Rev. Lett.*, 131:102501, Sep 2023. doi: 10.1103/PhysRevLett.131.102501. URL <https://link.aps.org/doi/10.1103/PhysRevLett.131.102501>.
- [78] Yu P Gangrsky, K P Marinova, S G Zemlyanoi, I D Moore, J Billowes, P Campbell, K T Flanagan, D H Forest, J A R Griffith, J Huikari, R Moore, A Nieminen, H Thayer, G Tungate, and J Äystö. Nuclear charge radii of neutron deficient titanium isotopes 44ti and 45ti. *Journal of Physics G: Nuclear and Particle Physics*, 30(9):1089, aug 2004. doi: 10.1088/0954-3899/30/9/009. URL <https://dx.doi.org/10.1088/0954-3899/30/9/009>.

- [79] Ross Mathieson. *Charge Radii Measurements of Chromium Nuclei by Laser Spectroscopy at IGISOL-IV*. PhD thesis, University of Liverpool, 2023.
- [80] F.C. Charlwood, J. Billowes, P. Campbell, B. Cheal, T. Eronen, D.H. Forest, S. Fritzsche, M. Honma, A. Jokinen, I.D. Moore, H. Penttilä, R. Powis, A. Saastamoinen, G. Tungate, and J. Äystö. Ground state properties of manganese isotopes across the  $n=28$  shell closure. *Physics Letters B*, 690(4):346–351, 2010. ISSN 0370-2693. doi: <https://doi.org/10.1016/j.physletb.2010.05.060>. URL <https://www.sciencedirect.com/science/article/pii/S0370269310006520>.
- [81] H. Heylen, C. Babcock, R. Beerwerth, J. Billowes, M. L. Bissell, K. Blaum, J. Bonnard, P. Campbell, B. Cheal, T. Day Goodacre, D. Fedorov, S. Fritzsche, R. F. Garcia Ruiz, W. Geithner, Ch. Geppert, W. Gins, L. K. Grob, M. Kowalska, K. Kreim, S. M. Lenzi, I. D. Moore, B. Maass, S. Malbrunot-Ettenauer, B. Marsh, R. Neugart, G. Neyens, W. Nörtershäuser, T. Otsuka, J. Papuga, R. Rossel, S. Rothe, R. Sánchez, Y. Tsunoda, C. Wraith, L. Xie, X. F. Yang, and D. T. Yordanov. Changes in nuclear structure along the mn isotopic chain studied via charge radii. *Phys. Rev. C*, 94:054321, Nov 2016. doi: 10.1103/PhysRevC.94.054321. URL <https://link.aps.org/doi/10.1103/PhysRevC.94.054321>.
- [82] K. Minamisono, D. M. Rossi, R. Beerwerth, S. Fritzsche, D. Garand, A. Klose, Y. Liu, B. Maaß, P. F. Mantica, A. J. Miller, P. Müller, W. Nazarewicz, W. Nörtershäuser, E. Olsen, M. R. Pearson, P.-G. Reinhard, E. E. Saperstein, C. Sumithrarachchi, and S. V. Tolokonnikov. Charge radii of neutron deficient  $^{52,53}\text{Fe}$  produced by projectile fragmentation. *Phys. Rev. Lett.*, 117:252501, Dec 2016. doi: 10.1103/PhysRevLett.117.252501. URL <https://link.aps.org/doi/10.1103/PhysRevLett.117.252501>.
- [83] Skyy V. Pineda, Kristian König, Dominic M. Rossi, B. Alex Brown, Anthony Incorvati, Jeremy Lantis, Kei Minamisono, Wilfried Nörtershäuser, Jorge Piekarewicz, Robert Powel, and Felix Sommer. Charge radius of neutron-deficient  $^{54}\text{Ni}$  and symmetry energy constraints using the difference in mirror pair charge radii. *Phys. Rev. Lett.*, 127:182503, Oct 2021. doi: 10.1103/PhysRevLett.127.182503. URL <https://link.aps.org/doi/10.1103/PhysRevLett.127.182503>.
- [84] Felix Sommer, Kristian König, Dominic M. Rossi, Nathan Everett, David Garand, Ruben P. de Groote, Jason D. Holt, Phillip Imgram, Anthony Incorvati, Colton Kalman, Andrew Klose, Jeremy Lantis, Yuan Liu, Andrew J. Miller, Kei Minamisono, Takayuki Miyagi, Witold Nazarewicz, Wilfried Nörtershäuser, Skyy V. Pineda, Robert Powel, Paul-Gerhard Reinhard, Laura Renth, Elisa Romero-Romero, Robert Roth, Achim Schwenk, Chandana Sumithrarachchi, and Andrea Teigelhöfer. Charge radii of  $^{55,56}\text{Ni}$  reveal a surprisingly similar behavior at  $n = 28$  in ca and ni isotopes. *Phys. Rev. Lett.*, 129:132501, Sep 2022. doi: 10.1103/PhysRevLett.129.132501. URL <https://link.aps.org/doi/10.1103/PhysRevLett.129.132501>.
- [85] M. L. Bissell, T. Carette, K. T. Flanagan, P. Vingerhoets, J. Billowes, K. Blaum, B. Cheal, S. Fritzsche, M. Godefroid, M. Kowalska, J. Krämer, R. Neugart, G. Neyens, W. Nörtershäuser, and D. T. Yordanov. Cu charge radii reveal a weak sub-shell effect at  $n = 40$ . *Phys. Rev. C*, 93:064318, Jun 2016. doi: 10.1103/PhysRevC.93.064318. URL <https://link.aps.org/doi/10.1103/PhysRevC.93.064318>.
- [86] L. Xie, X.F. Yang, C. Wraith, C. Babcock, J. Bieroń, J. Billowes, M.L. Bissell, K. Blaum, B. Cheal, L. Filippin, K.T. Flanagan, R.F. Garcia Ruiz, W. Gins, G. Gaigalas, M. Godefroid, C. Gorges, L.K. Grob, H. Heylen, P. Jönsson, S. Kaufmann, M. Kowalska, J. Krämer, S. Malbrunot-Ettenauer, R. Neugart, G. Neyens, W. Nörtershäuser, T. Otsuka, J. Papuga, R. Sánchez, Y. Tsunoda, and D.T. Yordanov. Nuclear charge radii of  $^{62-80}\text{Zn}$  and their dependence on cross-shell proton excitations. *Physics Letters B*, 797:134805, 2019. ISSN 0370-2693. doi: <https://doi.org/10.1016/j.physletb.2019.134805>. URL <https://www.sciencedirect.com/science/article/pii/S037026931930509X>.
- [87] T. J. Procter, J. Billowes, M. L. Bissell, K. Blaum, F. C. Charlwood, B. Cheal, K. T. Flanagan, D. H. Forest, S. Fritzsche, Ch. Geppert, H. Heylen, M. Kowalska, K. Kreim, A. Krieger, J. Krämer, K. M. Lynch, E. Mané, I. D. Moore, R. Neugart, G. Neyens, W. Nörtershäuser, J. Papuga, M. M. Rajabali, H. H. Stroke, P. Vingerhoets, D. T. Yordanov, and M. Žáková. Nuclear mean-square charge radii of  $^{63,64,66,68-82}\text{Ga}$  nuclei: No anomalous behavior at  $n = 32$ . *Phys. Rev. C*, 86:034329, Sep 2012. doi: 10.1103/PhysRevC.86.034329. URL <https://link.aps.org/doi/10.1103/PhysRevC.86.034329>.
- [88] G. J. Farooq-Smith, A. R. Vernon, J. Billowes, C. L. Binnersley, M. L. Bissell, T. E. Cocolios, T. Day Goodacre, R. P. de Groote, K. T. Flanagan, S. Franchoo, R. F. Garcia Ruiz, W. Gins, K. M. Lynch, B. A. Marsh, G. Neyens, S. Rothe, H. H. Stroke, S. G. Wilkins, and X. F. Yang. Probing the  $^{31}\text{Ga}$  ground-state properties in the region near  $z = 28$  with high-resolution laser spectroscopy. *Phys. Rev. C*, 96:044324, Oct 2017. doi: 10.1103/PhysRevC.96.044324. URL <https://link.aps.org/doi/10.1103/PhysRevC.96.044324>.

- [89] M. Keim, E. Arnold, W. Borchers, U. Georg, A. Klein, R. Neugart, L. Vermeeren, R.E. Silverans, and P. Lievens. Laser-spectroscopy measurements of 72–96kr spins, moments and charge radii. *Nuclear Physics A*, 586(2):219–239, 1995. ISSN 0375-9474. doi: [https://doi.org/10.1016/0375-9474\(94\)00786-M](https://doi.org/10.1016/0375-9474(94)00786-M). URL <https://www.sciencedirect.com/science/article/pii/037594749400786M>.
- [90] G. Fricke and K. Heilig. Nuclear charge radii · 36-kr krypton: Datasheet from landolt-börnstein - group i elementary particles, nuclei and atoms · volume 20: “nuclear charge radii” in springer materials ([https://doi.org/10.1007/10856314\\_38](https://doi.org/10.1007/10856314_38)), . URL [https://materials.springer.com/lb/docs/sm\\_lbs\\_978-3-540-45555-4\\_38](https://materials.springer.com/lb/docs/sm_lbs_978-3-540-45555-4_38). Copyright 2004 Springer-Verlag Berlin Heidelberg.
- [91] Tao Li, Yani Luo, and Ning Wang. Compilation of recent nuclear ground state charge radius measurements and tests for models. *Atomic Data and Nuclear Data Tables*, 140:101440, 2021. ISSN 0092-640X. doi: <https://doi.org/10.1016/j.adt.2021.101440>. URL <https://www.sciencedirect.com/science/article/pii/S0092640X21000267>.
- [92] G. Huber, C. Thibault, R. Klapisch, H. T. Duong, J. L. Vialle, J. Pinard, P. Juncar, and P. Jacquinet. High-resolution laser spectroscopy of the  $d$  lines of on-line produced  $^{21,22,24,25}\text{Na}$  using a new high-sensitivity method of detection of optical resonances. *Phys. Rev. Lett.*, 34:1209–1211, May 1975. doi: 10.1103/PhysRevLett.34.1209. URL <https://link.aps.org/doi/10.1103/PhysRevLett.34.1209>.
- [93] K Pescht, H Gerhardt, and E Matthias. Isotope shift and hfs of  $d$  1 lines in na-22 and 23 measured by saturation spectroscopy. *Zeitschrift für Physik A Atoms and Nuclei*, 281(3):199–204, 1977.
- [94] F. Touchard, J. M. Serre, S. Büttgenbach, P. Guimbal, R. Klapisch, M. de Saint Simon, C. Thibault, H. T. Duong, P. Juncar, S. Liberman, J. Pinard, and J. L. Vialle. Electric quadrupole moments and isotope shifts of radioactive sodium isotopes. *Phys. Rev. C*, 25:2756–2770, May 1982. doi: 10.1103/PhysRevC.25.2756. URL <https://link.aps.org/doi/10.1103/PhysRevC.25.2756>.
- [95] P. Plattner, E. Wood, L. Al Ayoubi, O. Beliuskina, M. L. Bissell, K. Blaum, P. Campbell, B. Cheal, R. P. de Groote, C. S. Devlin, T. Eronen, L. Filippin, R. F. García Ruíz, Z. Ge, S. Geldhof, W. Gins, M. Godefroid, H. Heylen, M. Hukkanen, P. Imgram, A. Jaries, A. Jokinen, A. Kanellakopoulos, A. Kankainen, S. Kaufmann, K. König, Á. Koszorús, S. Kujanpää, S. Lechner, S. Malbrunot-Ettenauer, P. Müller, R. Mathieson, I. Moore, W. Nörtershäuser, D. Nesterenko, R. Neugart, G. Neyens, A. Ortiz-Cortes, H. Penttilä, I. Pohjalainen, A. Raggio, M. Reponen, S. Rinta-Antila, L. V. Rodríguez, J. Romero, R. Sánchez, F. Sommer, M. Stryczyk, V. Virtanen, L. Xie, Z. Y. Xu, X. F. Yang, and D. T. Yordanov. Nuclear charge radius of  $^{26m}\text{Al}$  and its implication for  $v_{ud}$  in the quark-mixing matrix, 2023.
- [96] M. L. Bissell, J. Papuga, H. Naïdja, K. Kreim, K. Blaum, M. De Rydt, R. F. Garcia Ruiz, H. Heylen, M. Kowalska, R. Neugart, G. Neyens, W. Nörtershäuser, F. Nowacki, M. M. Rajabali, R. Sanchez, K. Sieja, and D. T. Yordanov. Proton-neutron pairing correlations in the self-conjugate nucleus  $^{38}\text{K}$  probed via a direct measurement of the isomer shift. *Phys. Rev. Lett.*, 113:052502, Jul 2014. doi: 10.1103/PhysRevLett.113.052502. URL <https://link.aps.org/doi/10.1103/PhysRevLett.113.052502>.
- [97] E. Mané, A. Voss, J. A. Behr, J. Billowes, T. Brunner, F. Buchinger, J. E. Crawford, J. Dilling, S. Ettenauer, C. D. P. Levy, O. Shelbaya, and M. R. Pearson. First experimental determination of the charge radius of  $^{74}\text{Rb}$  and its application in tests of the unitarity of the cabibbo-kobayashi-maskawa matrix. *Phys. Rev. Lett.*, 107:212502, Nov 2011. doi: 10.1103/PhysRevLett.107.212502. URL <https://link.aps.org/doi/10.1103/PhysRevLett.107.212502>.